ANL-77-3

ANL-77-3



# THEORETICAL STUDIES OF THE ATMOSPHERIC TRIATOMIC MOLECULES $H_2O$, $N_2O$, $NO_2$, $CO_2$, $O_3$, AND THEIR IONS

by

Arnold C. Wahl, Walter B. England,
Bruce J. Rosenberg, Darrel G. Hopper,
and Patrick J. Fortune

U of C-AUA-USERDA

ARGONNE NATIONAL LABORATORY, ARGONNE, ILLINOIS

Operated for the U. S. ENERGY RESEARCH
AND DEVELOPMENT ADMINISTRATION
under Contract W-31-109-Eng-38

Printed in the United States of America
Available from
National Technical Information Service
U. S. Department of Commerce
5285 Port Royal Road
Springfield, Virginia 22161
Price: Printed Copy $4.50; Microfiche $3.00

Distribution Category:
Chemistry (UC-4)

ANL-77-3



ARGONNE NATIONAL LABORATORY
9700 South Cass Avenue
Argonne, Illinois 60439



# THEORETICAL STUDIES OF THE ATMOSPHERIC TRIATOMIC MOLECULES $H_2O$, $N_2O$, $NO_2$, $CO_2$, $O_3$, AND THEIR IONS

by

Arnold C. Wahl
Principal Investigator

and

Walter B. England, Bruce J. Rosenberg,
Darrel G. Hopper, and Patrick J. Fortune
Project Scientists

Chemistry Division

Annual Report on Research Performed under
Air Force Contracts AFOSR-ISSA-76-0003
and
AFOSR-ISSA-7T-0001 (ANL Proposal P-7510-A)

Reporting Period: July 1, 1975—September 31, 1976

TABLE OF CONTENTS

# INTRODUCTION

The molecules $H_2O$, $NO_2$, $O_3$, $CO_2$ and $N_2O$ are the dominant triatomic species in the earth's atmosphere. Because of the ready availability of high energy electromagnetic radiation in the upper atmosphere their behavior can be quite diverse. Absorption processes leave the molecules in highly excited and ionized states, and in these cases geometries often differ drastically from the ground state geometries. Furthermore, dissociation and predissociation to atom-diatom asymptotes is common. In order to understand such atmospheric processes, certain fundamental quantities are needed; among these are the definitive location of the excited energy levels and the delineation of reaction mechanisms. These same quantities clearly are necessary for describing the basic chemical behavior of these molecules. In spite of this need, most existing information is inadequate for interpretive or predictive purposes, and understanding atmospheric reactions remains largely guesswork. Our investigation is concerned with providing these energy levels and reaction surfaces through the use of well established *ab initio* techniques. This new theoretical knowledge will be used to advance experimental analysis by participating in a feedback process which historically has proved to provide a deeper understanding of the phenomena involved. We hope that the foundation established by this research will lead to an expanded effort in atmospheric computations at Argonne. Our concerns the past year have largely been excited state characterization and method calibration. Both are prerequisites for any long-range investigation. This is particularly true of the air triatomics because there is so little definitive information presently available. We have also determined linear geometry to bent geometry correlation diagrams. These provide simple ways of predicting reaction possibilities. For example, we found that the four lowest excited states of $CO_2^+$ are most stable in linear geometries. The fifth excited state was found to be more stable in a bent geometry. Moreover, in the bent geometry it becomes more stable than three of the four lowest linear ion states, and hence, very likely predissociates the lower energy linear states of $CO_2^+$. It is probable that the predissociation just described for $CO_2^+$ carries over into the Rydberg series that ultimately converge to the ion states in question. Both types of predissociation could be important in atmospheric processes. There are numerous similar examples of important information being provided by this theoretical study.

We have used a variety of quantum chemistry computational techniques in our study of the atmospheric triatomic molecules. Certainly, an integral part of our systematic study is the calibration of various levels and methods of computation. The computational methods used here include: (1) expansion or Roothan self-consistent field (SCF)[1], (2) traditional configuration interaction (CI) using canonical molecular orbitals[2], (3) multi-configuration self-consistent field/configuration interaction (MCSCF/CI)[3,4,5], and (4) equations-of-motion (EOM)[6]. The computer ccdes used in our study were (1) the BISONMC[7] program developed by Das and Wahl for computing SCF and MCSCF wavefunctions, (2) the Battelle-Ohio State CI package developed by Shavitt and co-workers, and (3) the EOM programs developed by McKoy and co-workers at Caltech. The following subsections consist of a molecule-by-molecule summary of the results which are the body of this report.

$\underline{H_2O}$. $H_2O^+$ is the simplest prototype for ion-molecule reactions among the air triatomics. We have computed potential energy surfaces for the ground $^2B_1$ and the $^2B_2$ states of $H_2O^+$. The results of our vibrational analysis of the $^2B_1$ surface are in good agreement with experiment. The $^2B_2$ surface is thought to be predissociated twice, and has a complicated anharmonic vibrational structure. The present level of our results support either of two experimental claims regarding the band origins.

$\underline{CO_2}$. Previous theoretical spectra were shown to be of limited accuracy. Experimental assignments based on these are therefore not definitive. Our best correlated spectra are the most accurate available for the lowest multiplet of $CO_2$. Linear geometry to bent geometry correlation diagrams were also determined for the $CO_2$, $CO_2^+$ and $CO_2^-$ systems. Excited states of $CO_2$ were found to be stable in bent geometries relative to atom-diatom dissociation. Several of the excited linear states in $CO_2^+$ are likely to predissociate via a lower-lying bent geometry state. Conflicts with existing $CO_2^-$ level assignments were found, and the spectrum was reassigned. Finally, the character of vertically excited states in neutral $CO_2$ was determined.

$\underline{O_3}$. The ongoing controversy over the reaction of ozone with photolyzed freons underlines the important role these triatomics play in atmospheric chemistry. Our correlated results for the vertical excitation energies of $O_3$ are in very good agreement with experiment, and with other calculations. The $O_3^+$ and $O_3^-$ calculations provide qualitatively correct electronic spectra for the ions. The ordering of states in $O_3^+$ is controversial at present, and we support the ordering $X^2A_1$, $A^2B_2$ and $B^2A_2$. Our $O_3^-$ spectrum is the only existing data concerning the excitation energies of this ion.

$\underline{N_2O}$. The ground state potential energy surface of $N_2O^-$ is characterized and related to the ground state potential energy surface of the neutral $N_2O$ molecule by combining theoretical and experimental information. Among the quantities reported are equilibrium geometries, dissociation energies, vertical and adiabatic electron affinities, and the minimum intersection locus of the ground state $N_2O$ and $N_2O^-$ surfaces. The results imply that the reaction $O^- + N_2 \rightarrow N_2O + e$ will be strongly enhanced by $N_2$ vibrational excitation.

$\underline{NO_2}$. A definitive theoretical study of $NO_2$[5] was performed earlier in our laboratory. Agreement with known experimental results was very good. The energy levels obtained in our present effort provide similar data for $NO_2^+$ and $NO_2^-$, where little reliable information is available. Agreement with our previous $NO_2$ study[5] is good. We suggest that known spectral complexities in $NO_2^+$ are due to vibrationally excited states. We also found that existing theoretical $NO_2^+$ spectra do not consider all of the electronic states in their reported energy ranges, and hence, spectral assignments based on these are unreliable. Our $NO_2^-$ energy levels are the only existing *ab initio* information.

Part of our computational efforts were supported by the CDC6600 computers at Wright-Patterson Air Force Fase. We discuss our experience performing large scale molecular calculations remotely on the Wright-Patterson computers in Reference 8 of the publication list given in the next section. Many elements of the effort are general and can be expected to be encountered by other researchers. A summary of the historically important role played by Wright-Patterson is also given.

Personnel Changes. At the end of the last fiscal year, Dr. Richard C. Raffenetti replaced Dr. P. J. Fortune (who joined the staff of the Applied Mathematics Division at Argonne) as project scientist on the Atmospheric Triatomic Molecules project. Dr. Raffenetti received his Ph.D. in physical chemistry from Iowa State University in 1971. He subsequently held post-doctoral appointments at Battelle Memorial Institute and Johns Hopkins University, and most recently was a visiting scientist at the Institute for Computer Applications in Science and Engineering, located at the NASA Langley Research Center.

Acknowledgements. We wish to thank Drs. W. C. Ermler and D. L. Yeager of the University of Chicago for their kind collaboration. We are also grateful to Professor T. O. Tiernan and Dr. R. L. C. Wu of Wright State University for their stimulating experimental collaboration.

REFERENCES


1. C. C. J. Roothaan, Rev. Mod. Phys. **23**, 69 (1951); ibid. **32**, 179 (1960); C. C. J. Roothaan and P. S. Bagus, "Methods in Computational Physics, Vol. 2", B. Alder, S. Fernbach and M. Rotenberg, eds. (Academic Press, New York, 1963).

2. I. Shavitt, "Modern Theoretical Chemistry. Vol. 3, Methods of Electronic Structure Theory," H. F. Schaefer III, ed. (Plenum Publishing Corp. New York, 1977).

3. A. C. Wahl and G. Das, "Modern Theoretical Chemistry. Vol. 3, Methods of Electronic Structure Theory," H. F. Schaefer III, ed. (Plenum Publishing Corp. New York, 1977).

4. F. P. Billingsley II, J. Chem. Phys. **62**, 864 (1975); ibid. **63**, 2267 (1975).

5. G. D. Gillispie, A. U. Khan, A. C. Wahl, R. P. Hosteny, and M. Krauss, J. Chem. Phys. **63**, 3425 (1975).

6. C. W. McCurdy, Jr., T. N. Rescigno, D. L. Yeager, and V. McKoy, "Modern Theoretical Chemistry. Vol. 3, Methods of Electronic Structure Theory," H. F. Schaefer III, ed. (Plenum Publishing Corp., New York, 1977).

7. G. Das and A. C. Wahl, "BISONMC: A FORTRAN Computing System for Multiconfiguration Self-Consistent Field (MCSCF) Calculations on Atoms, Diatoms, and Polyatoms," Argonne National Laboratory Report ANL-7955, 1972.

# PUBLICATION LIST

Most of the results described in this report have been published or submitted for publication in the open literature. These papers should be consulted for further details and for discussions of the theoretical methods employed. For convenience, we have assembled a collection of these works which is available upon request from the authors. A list of the papers in question follows.


1. Theoretical Studies of Atmospheric Molecules: SCF and Correlated Potential Surface Results for the $X^2B_1$ and $\tilde{B}^2B_2$ States of $H_2O^+$, J. Chem. Phys. 65, 2201 (1976).

2. *Ab Initio* Vertical Spectra and Linear-Bent Correlation Diagrams for the Valence States of $CO_2$ and Its Singly-Charged Ions, J. Chem. Phys. 65, 684 (1976).

3. Theoretical Studies of Atmospheric Triatomic Molecules: Accurate SCF Vertical Spectrum for Valence, Mixed Character, and Rydberg States of $CO_2$, J. Chem. Phys., March 1977.

4. Theoretical Studies of Atmospheric Triatonia Molecules: *Ab Initio* Equations of Motion Excitation Energies for Valence States of the Configuration $1\pi_g^3\ 2\pi_u^1$ in $CO_2$, J. Chem. Phys., March 1977.

5. Theoretical Studies of Atmospheric Molecules: *Ab Initio* Vertical Spectra for the Valence States of Ozone and Its Singly-Charged Ions, preprint.

6. Theoretical and Experimental Studies of the $N_2O^-$ and $N_2O$ Ground State Potential Energy Surfaces. Implications for the $O^- + N_2 = N_2O + e$ and Other Processes, J. Chem. Phys., 65, 5475 (1976).

7. Theoretical Studies of Atmospheric Molecules: SCF and Correlated Energy Levels for the $NO_2$, $NO_2^+$ and $NO_2^-$ Systems, Theor. Chim. Acta. submitted.

PUBLICATION LIST, CONT'D.

8. A Case History in Computer Resource Sharing: *Ab Initio* Calculations Via a Remote Terminal, "Computer Networks and Chemistry," P. Lykos, ed. (ACS Publications, Washington, 1975).

# WATER AND ITS POSITIVE ION

## A. Introduction

The equilibrium geometry of the $X^1A_1$ state of $H_2O$ has been determined by infrared spectroscopy,[1] and various empirical determinations of the internal coordinate force constants have been derived from perturbation analyses of the spectroscopic data.[2,3,4] The deficiencies in the potential energy constants obtained from *ab initio* self-consistent-field (SCF) calculations are apparent from the resultant computed vibrational energies.[5,6]

Experimental equilibrium geometries have been obtained for the $X^2B_1$, $1^2A_1$, and $1^2B_2$ states of $H_2O$,[7-10] but no determinations of potential energy constants have been made yet. Potential energy surfaces for the ground and several excited states of $H_2O^+$ have been computed using *ab initio* SCF and semi-empirical configuration interaction (CI) techniques.[11] The theoretical results[11] and photoelectron spectra[12,13] were subsequently combined to discuss the predissociation and analyze the vibrational structure of the $1^2B_2$ state, and it was concluded that the $^2B_2$ state was predissociated twice.[9] The position of the appearance potential of the $OH^+$ ion being just above the $1^2B_2$ adiabatic ionization potential is also related to the predissociation of the upper vibrational levels of that state. The coupling of the $1^2B_2$ and $1^2A_1$ components of the $1^2A'$ state adds to the complexity of the $^2B_2$ surface.

## B. Neutral $H_2O$

One of the authors (BJR) has previously computed *ab initio* SCF and CI potential energy surfaces in the neighborhood of the energy minimum for the $X^1A_1$ state of $H_2O$.[14] The energy surface was represented by a quartic Taylor series expansion, in terms of the internal coordinates ($\Delta R_1$, $\Delta R_2$, $\Delta\theta$), of the form[6]

$$
\begin{aligned}
E = E_e &+ K_4(\Delta R_1^2 + \Delta R_2^2) + K_5\Delta\theta^2 + 2K_6\Delta R_1\Delta R_2 \\
&+ 2K_7(\Delta R_1 + \Delta R_2)\Delta\theta + K_8(\Delta R_1^3 + \Delta R_2^3) + K_9\Delta\theta^3 \\
&+ 3K_{10}(\Delta R_1 + \Delta R_2)\Delta R_1\Delta R_2 + 3K_{11}(\Delta R_1^2 + \Delta R_2^2)\Delta\theta \\
&+ 6K_{12}\Delta R_1\Delta R_2\Delta\theta + 3K_{13}(\Delta R_1 + \Delta R_2)\Delta\theta^2 \\
&+ K_{14}(\Delta R_1^4 + \Delta R_2^4) + K_{15}\Delta\theta^4 + 4K_{16}(\Delta R_1^2 + \Delta R_2^2)\Delta R_1\Delta R_2 \\
&+ 6K_{17}\Delta R_1^2\Delta R_2^2 + 4K_{18}(\Delta R_1^3 + \Delta R_2^3)\Delta\theta \\
&+ 12K_{19}(\Delta R_1 + \Delta R_2)\Delta R_1\Delta R_2\Delta\theta + 6K_{20}(\Delta R_1^2 + \Delta R_2^2)\Delta\theta^2 \\
&+ 12K_{21}\Delta R_1\Delta R_2\Delta\theta^2 + 4K_{22}(\Delta R_1 + \Delta R_2)\Delta\theta^3 \qquad (1)
\end{aligned}
$$

The resultant force constants along with various empirically-derived sets are given in Table I. Recently, in collaboration with workers at other laboratories, these potential energy constants have been used in a variation-perturbation method[6] to compute vibrational energy levels.[15] The calculated and experimentally-observed[1] energy levels are compared in Table II. The importance of including correlation effects in the wavefunction when computing potential energy surfaces is evident from the significant improvement in the CI harmonic force constants ($K_4$-$K_7$) and vibrational energies compared to the SCF values. The CI vibrational energies show an average error of $\sim$ 4%.

C. Positive Ion $H_2O^+$

*Ab initio* SCF and multi-configuration self-consistent field/configuration interaction (MCSCF/CI) potential energy surfaces, in the neighborhood of the energy minima, were computed for the $X^2B_1$ and $\tilde{B}^2B_2$ states of $H_2O^+$. The energies were fit to a cubic Taylor series expansion (Eq. (1), truncated after $K_{13}$), and the resulting equilibrium geometries and force constants are presented in Table III. The computed equilibrium geometries are seen to be consistent with what one would expect from Walsh's rules. The potential energy constants were then input to a vibrational analysis program[6] to compute harmonic frequencies, Table IV, and second-order corrected vibrational energies, Table V.

From Table V, it is clear that the computed vibrational results for the $^2B_1$ state are in good agreement with available experimental data.[7,12,13,16] However, it is seen that the lowest symmetric and asymmetric stretching frequencies are stable to only about 10% as one proceeds from the harmonic to cubic fits, i.e., Table IV to Table V; the lowest bending frequency changes very little which is consistent with the fact that the dominant cubic term is $K_8$.

The results for all the vibrational frequencies of the $^2B_2$ state exhibit significant changes as the effects of cubic terms are added. This is to be expected at the outset, as the anharmonic nature of the progression of peaks in the photoelectron spectrum has been observed.[13] It is interesting to note that the value quoted in Ref. 13 for the lowest bending excitation agrees with that from the cubic analysis, while the harmonic results agree with those of Ref. 12.

### D. Future Goals

Because of the marked changes in the vibrational energies on including cubic anharmonic terms in the potential energy expansion, it is necessary to investigate the effects of adding quartic and higher terms in the expansion. In an attempt to resolve the disputed assignments of the $^2B_2$ band origins of the photoelectron spectra of $H_2O$, higher order perturbation theory, or a variational approach[17,18] will also be considered.

In order to study the predissociation of the $^2B_2$ state, it will be necessary to compute potential surfaces for the $1^4A''$ and $2^2A''$ states as well as additional regions of the $^2B_2$ surface. A complete understanding of the $^2B_2$ state will also require an examination of its coupling through asymmetric distortion with the $1^2A_1$ state.

## REFERENCES


1. W. S. Benedict, N. Gailar, and E. K. Plyler, J. Chem. Phys. 24, 1139 (1956).

2. K. Kuchitsu and Y. Morino, Bull. Chem. Soc. Japan 38, 814 (1965).

3. D. F. Smith and J. Overend, Spectrochim. Acta 28A, 471 (1972).

4. A. R. Hoy, I. M. Mills, and G. Strey, Mol. Phys. 24, 1265 (1972).

5. W. C. Ermler and C. W. Kern, J. Chem. Phys. 55, 4851 (1971).

6. B. J. Krohn, W. C. Ermler, and C. W. Kern, J. Chem. Phys. 60, 22 (1974).

7. H. Lew and I. Heiber, J. Chem. Phys. 58, 1246 (1973).

8. T. E. Sharp and H. M. Rosenstock, J. Chem. Phys. 41, 3453 (1964); V. H. Dibeler, J. A. Walker, and H. M. Rosenstock, J. Res. Nat. Bur. Std. A70, 459 (1966); R. Botter and H.M. Rosenstock, "International Conference of Mass Spectrometry, Advances in Mass Spectrometry, Vol. 4", 1967; R. Botter and H. M. Rosenstock, J. Res. Nat. Bur. Std. A73, 313 (1969).

9. A. J. Lorquet and J. C. Lorquet, Chem. Phys. 4, 353 (1974).

10. F. Erman and J. Bryozowski, Phys. Lett. 46A, 79 (1973).

11. J. C. Leclerc, J. A. Horsley, and J. C. Lorquet, Chem. Phys. 4, 337 (1974).

12. C. R. Brundle and D. W. Turner, Proc. Roy. Soc. London A307, 27 (1968).

13. A. W. Potts and W. C. Price, Proc. Roy. Soc. London A326, 181 (1972).

14. B. J. Rosenberg, W. C. Ermler, and I. Shavitt, J. Chem. Phys. 65, 4072 (1976).

15. W. C. Ermler, B. J. Rosenberg, and I. Shavitt, in preparation.

16. L. Karlsson, L. Mattsson, R. Jadrny, R. G. Albridge, S. Pinchas, T. Bergmark, and K. Siegbahn, J. Chem. Phys. 62, 4745 (1975).

17. R. J. Whitehead and N. C. Handy, J. Mol. Spectrosc. 55, 356 (1975); ibid 59, 459 (1976).

18. G. D. Carney and C. W. Kern, Int. J. Quantum Chem. S9, 317 (1975).

Table I. Equilibrium Geometry and Force Constants for the $X^1A_1$ State of the Water Molecule[a]

| Constant | SCF[b] | CI[b] | SO[c] | KM(I)[d] | KM(II)[d] | HMS[e] |
|---|---|---|---|---|---|---|
| $R_e$ | 1.77604 | 1.80040 | 1.8089 | 1.8089 | 1.8089 | 1.8089 |
| $\theta_e$ | 106.085° | 104.930° | 104.52° | 104.52° | 104.52° | 104.52° |
| $E_e$ | -76.06497650(2) | -76.33986662(2) | - | - | - | - |
| $K_4$ | 0.31451(3) | 0.28504(1) | 0.271(1) | 0.2715 | 0.2715 | 0.2715 |
| $K_5$ | 0.088652(6) | 0.084685(8) | 0.085(4) | 0.0800 | 0.0800 | 0.0799 |
| $K_6$ | -0.00212(2) | -0.002661(9) | -0.004(1) | -0.0032 | -0.0032 | -0.0032 |
| $K_7$ | 0.014695(3) | 0.015655(4) | 0.029(9) | 0.0132 | 0.0132 | 0.0133 |
| $K_8$ | -0.3745(6) | -0.3462(2) | -0.33(2) | -0.339(2) | -0.36(2) | -0.34(5) |
| $K_9$ | -0.03022(8) | -0.02711(4) | -0.045(3) | -0.029(2) | -0.027(4) | -0.03(1) |
| $K_{10}$ | 0.0000(2) | -0.00025(6) | -0.002(6) | -0.004(2) | 0.006(6) | 0.00(3) |
| $K_{11}$ | -0.0007(3) | -0.0008(1) | -0.01(1) | 0.0034(6) | 0.005(1) | 0.004(6) |
| $K_{12}$ | -0.0057(3) | -0.0055(1) | -0.007(4) | -0.0071(1) | -0.0049(4) | -0.004(9) |
| $K_{13}$ | -0.00602(3) | -0.00601(2) | -0.017(1) | 0.006(8) | 0.01(1) | -0.004(6) |

| Constant | SCF[b] | CI[b] | SO[c] | KM(I)[d] | KM(II)[d] | HMS[e] |
|---|---|---|---|---|---|---|
| $K_{14}$ | 0.277(3) | 0.277(4) | 0.27(7) | 0.302(6) | 0.36(3) | 0.3(1) |
| $K_{15}$ | -0.0094(5) | -0.0069(6) | -0.01(3) | 0.00(4) | 0.00(4) | -0.001(6) |
| $K_{16}$ | -0.0004(6) | -0.0001(8) | 0.006(8) | 0.004(3) | -0.01(1) | -0.00(4) |
| $K_{17}$ | 0.0004(5) | 0.0004(6) | 0.007(7) | 0.004(4) | 0.00(1) | 0.00(2) |
| $K_{18}$ | -0.002(3) | -0.002(3) | -0.06(6) | - | - | - |
| $K_{19}$ | 0.0005(9) | 0.001(1) | -0.02(3) | - | - | - |
| $K_{20}$ | -0.0009(6) | -0.0008(7) | -0.01(2) | -0.018(9) | -0.03(1) | -0.0037(6 |
| $K_{21}$ | 0.0015(5) | 0.0017(6) | -0.00(2) | -0.003(9) | -0.01(1) | 0.001(4) |
| $K_{22}$ | 0.0036(1) | 0.0031(2) | -0.01(3) | - | - | - |

[a] All quantities in atomic units, and are referred to Eq. (1).

[b] B. J. Rosenberg, W. C. Ermler, and I. Shavitt, J. Chem. Phys. 65, 4072 (1976). Error limits, in parenthesis, are 3 x statistical standard deviations in the last significant digit.

[c] D. F. Smith and J. Overend, Spectrochimica Acta 28A, 471 (1972). Error limits, in parenthesis, are 3 x statistical standard deviations in the last significant digit.

[d] K. Kuchitsu and Y. Morino, Bull. Chem. Soc. Japan 38, 814 (1965). Error limits, in parenthesis, are 3 x uncertainties in the last significant digit. Constants $K_{18}$, $K_{19}$ and $K_{22}$ were constrained to be zero. Columns (I) and (II) are anharmonic force constants for $H_2O$ and $D_2O$, respectively.

[e] A. R. Hoy, I. M. Mills and G. Strey, Mol. Phys. 24, 1265 (1972). Error limits, in parenthesis, are the estimated uncertainties in the last significant digit. Constants $K_{18}$, $K_{19}$ and $K_{22}$ were constrained to be zero.

Table II. Energies of low-lying vibrational states of the $X\,^1A_1$ state of $H_2O$[a].

| Vibrational State[b] | SCF | CI | Expt.[c] |
|---|---|---|---|
| (0,0,0) | 5008 | 4777 | 4634 |
| (1,0,0) | 8968 | 8537 | 8290 |
| (0,1,0) | 6757 | 6463 | 6231 |
| (0,0,1) | 9077 | 8646 | 8388 |
| (2,0,0) | 12842 | 12212 | 11861 |
| (0,2,0) | 8473 | 8120 | 7794 |
| (0,0,2) | 13053 | 12422 | 12048 |
| (1,1,0) | 10716 | 10223 | 9871 |
| (1,0,1) | 12866 | 12339 | 11879 |
| (0,1,1) | 10849 | 10354 | 9965 |

[a]All energies in $cm^{-1}$.

[b]The vibrational modes are labeled in the standard fashion, i.e., 1-2-3 correspond to symmetric stretch - bend - asymmetric stretch, respectively.

[c]W. S. Benedict, N. Gailar, and E. K. Plyler, J. Chem. Phys. **24**, 1139 (1956).

Table III. Equilibrium geometry and force constants for the $X^2B_1$ and $\tilde{B}^2B_2$ states of $H_2O^+$.[a]

| Constant | $X^2B_1$ SCF | $X^2B_1$ MCSCF/CI | $\tilde{B}^2B_2$ SCF | $\tilde{B}^2B_2$ MCSCF/CI |
|---|---|---|---|---|
| $R_e$ | 1.8624 | 1.9037 | 2.0846 | 2.1544 |
| $\theta_e$ | 111.41° | 108.50° | 58.45° | 54.96° |
| $E_e$ | -75.645647(1) | -75.723280(1) | -75.476289(8) | -75.55451(1) |
| $K_4$ | 0.241(2) | 0.2111(7) | 0.114(5) | 0.092(5) |
| $K_5$ | 0.0725(7) | 0.0742(2) | 0.120(2) | 0.152(2) |
| $K_6$ | 0.002(1) | -0.0007(5) | 0.026(4) | 0.020(3) |
| $K_7$ | 0.0073(7) | 0.0088(2) | 0.029(2) | 0.034(1) |
| $K_8$ | -0.257(9) | -0.25(1) | -0.13(8) | -0.1(2) |
| $K_9$ | -0.029(3) | -0.028(4) | -0.18(3) | -0.21(4) |
| $K_{10}$ | 0.000(2) | 0.000(3) | -0.01(2) | -0.01(5) |
| $K_{11}$ | -0.00(1) | -0.01(1) | -0.0(1) | -0.01(4) |
| $K_{12}$ | -0.004(8) | 0.00(1) | -0.01(8) | -0.00(2) |
| $K_{13}$ | -0.007(3) | -0.006(4) | -0.05(3) | -0.05(2) |

[a]All quantities in atomic units and are referred to Eq. (1). Numbers in parenthesis following force constant values are three times the statistical standard deviation in the last digit reported.

| Frequency | $X\,^2B_1$ | | $\tilde{B}\,^2B_2$ | |
|---|---|---|---|---|
| | SCF | MCSCF/CI | SCF | MCSCF/CI |
| $\omega_1$ | 3635 | 3388 | 2872 | 2651 |
| $\omega_2$ | 1538 | 1518 | 1617 | 1669 |
| $\omega_3$ | 3685 | 3469 | 2178 | 1975 |

[a] All frequencies in $cm^{-1}$.

Table V. Energies of low-lying vibrational states of the $X^2B_1$ and $\tilde{B}^2B_2$ states of $H_2O^+$.[a]

| Vibrational State[b] | $X^2B_1$ SCF | $X^2B_1$ MCSCF/CI | $\tilde{B}^2B_2$ SCF | $\tilde{B}^2B_2$ MCSCF/CI |
|---|---|---|---|---|
| (0,0,0) | 4321 | 4054 | 3152 | 3009 |
| (1,0,0)[c,d,e] | 7687 | 7102 | 5512 | 5303 |
| (0,1,0)[c,d,e,f] | 5829 | 5543 | 4510 | 4473 |
| (0,0,1) | 7726 | 7172 | 4994 | 4742 |
| (2,0,0) | 10922 | 9982 | 7737 | 7489 |
| (0,2,0) | 7312 | 7013 | 5848 | 5920 |
| (0,0,2) | 10988 | 10115 | 6728 | 6386 |
| (1,1,0) | 9185 | 8584 | 6482 | 6484 |
| (1,0,1) | 10819 | 9882 | 6989 | 6821 |
| (0,1,1) | 9226 | 8650 | 6261 | 6114 |

[a]All energies in $cm^{-1}$.

[b]Vibrational modes are labeled in the standard fashion, i.e., 1-2-3 correspond to symmetric stretch-bend-asymmetric stretch, respectively.

[c]C.R. Brundle and D.W. Turner, Proc. Roy. Soc. London A307, 27 (1968). Excitation energies from (0,0,0) are: $\Delta E(1,0,0) = 3200\ cm^{-1}$, $\Delta E(0,1,0) = 1380\ cm^{-1}$ for $X^2B_1$ state, and $\Delta E(1,0,0) = 2990\ cm^{-1}$, $\Delta E(0,1,0) = 1610\ cm^{-1}$ for $\tilde{B}^2B_2$ state.

[d]A.W. Potts and W.C. Price, Proc. Roy. Soc. London A326, 181 (1972). Excitation energies from (0,0,0) are $\Delta E(1,0,0) = 3220\ cm^{-1}$, $\Delta E(0,1,0) = 1370\ cm^{-1}$ for $X^2B_1$ state, and $\Delta E(1,0,0) = 2985\ cm^{-1}$, $\Delta E(0,1,0) = 1370\ cm^{-1}$ for $\tilde{B}^2B_2$ state.

[e]L. Karlsson, L. Mattsson, R. Jadrny, R. G. Albridge, S. Pinchas, T. Bergmark, and K. Siegbahn, J. Chem. Phys. 62, 4745 (1975). Excitation Energies from (0,0,0) are $\Delta E(1,0,0) = 3242\ cm^{-1}$, $\Delta E(0,1,0) = 1428\ cm^{-1}$ for $X^2B_1$ state, and $\Delta E(1,0,0) = 2928\ cm^{-1}$, $\Delta E(0,1,0) = 1524\ cm^{-1}$ for $\tilde{B}^2B_2$ state.

[f]H. Lew and I. Heiber, J. Chem. Phys. 58, 1246 (1973). Excitation energy from (0,0,0) is $\Delta E(0,1,0) = 1412\ cm^{-1}$ for $X^2B_1$ state.

# CARBON DIOXIDE AND ITS IONS

## A. Introduction

Simple Walsh-Mulliken predictions[1,2] anticipate much of the interesting and varied behavior of the $CO_2$, $CO_2^+$, $CO_2^-$ molecules in a qualitative sense. A linear equilibrium geometry is predicted for ground state $CO_2$, while many of the low-lying excited states of $CO_2$ are predicted to be bent. Under these conditions, the electronic spectrum and possible attachment, detachment, dissociation, etc., mechanisms may very widely with geometry. A similar prediction is made for $CO_2^+$. In $CO_2^+$, however, there should also be many low-lying and as yet unobserved states which arise from the large number of unoccupied molecular orbitals. The negative ion $CO_2^-$ is predicted to have a bent equilibrium geometry. Again because of the large number of unoccupied valence molecular orbitals, many low-lying excited states are anticipated. A large number of these are expected to be resonance states, inasmuch as $CO_2$ will not bind an electron in many cases.

Apart from qualitative considerations such as those just outlined, rather little information exists concerning the electronic states of the $CO_2/CO_2^+/CO_2^-$ systems. Definitive information consists of Dixon's assignment[3,4] of the $1\ ^1B_2 \leftarrow 1\ ^1A_1$ transition in $CO_2$, and the four lowest vertical ionization potentials of $CO_2$.[5] Rydberg series in $CO_2$ have also been accurately measured,[6] but the nature of the Rydberg orbitals involved, and hence the symmetry of the electron states, is unknown. The lower-lying electronic states of $CO_2$ are complicated by the possibility of valence-Rydberg mixing, and almost nothing is known about these states. Even the lowest valence type states have not been definitely analyzed experimentally, and existing theoretical investigations[7,8] of these states have not employed sufficient accuracy for the results to be accepted without question.

With the exception of a semiempirical study,[9] little theoretical work has been done on the electronic states of $CO_2^-$. Subsequent *ab initio* work[10,11] has shown the semiempirical results to be even qualitatively incorrect as regards the stability of ground state $CO_2^-$ relative to ground state $CO_2$. The semiempirical model predicted that the ground state potential energy surfaces of $CO_2$ and $CO_2^-$ do not intersect, whereas *ab initio*[10,11] and experimental[12] findings showed that the surfaces do intersect. As a consequence, the assignments based on the semiempirical model are open to questions.

B. Linear and Bent Geometry Correlation Diagrams

The changes in the $CO_2/CO_2^+/CO_2^-$ electronic states upon molecular bending were determined by two sets of computations. First, self-consistent-field (SCF) calculations were carried out at the equilibrium bondlength ($R_{CO}$=2.1944 bohrs) of ground state $CO_2(X^1\Sigma_g^+)$. Second, the bondlength $R_{CO}$ was held fixed, and SCF calculations performed at a bond angle close to estimates[11,12] of the equilibrium bond angle of ground state $CO_2^-$ $(X^2A_1)$, $\sphericalangle$ OCO = 130°. Results for both geometries were obtained for each of the molecules $CO_2/CO_2^+/CO_2^-$.

Neutral $CO_2$

Figure 1 shows the linear and bent geometry spectra for the lowest-lying valence states of $CO_2$. Most of the excited states shown will have minimal energies for bent geometries. Electronic spectra which involve bent geometry $CO_2$ molecules will be clearly very different from the vertical (linear geometry) spectrum of $CO_2$. The bent molecule energy levels support Dixon's assignment of $B_2$ symmetry.[3,4] A total of five bent states ($^1A_1$, $^3B_2$, $^3A_2$, $^1A_2$, $^1B_2$) are bound relative to the lowest SCF asymptote, $CO(^1\Sigma^+) + O\ (^3P)$. The diagram partially supports an earlier mechanism[13] for the reaction

$$O(^3P) + CO(^1\Sigma^+) \rightarrow CO_2(^1\Sigma_g^+) \qquad (1)$$

in which the surfaces $^1B_2$ and $^3B_2$ are assumed to cross, and partially supports a mechanism[14] in which the two surfaces are not assumed to cross. In terms of the former mechanism, the predicted $^1B_2$ surface appears to overestimate the well depth.[4] A binding energy of $\sim$2 eV is predicted for $^3B_2$ relative to $O(^3P) + CO(^1\Sigma^+)$, and this concurs with both earlier kinetic studies.[13,14]

## Positive Ion $CO_2^+$

Figure 2 shows the linear-bent correlation diagram for $CO_2^+$. Known and unknown excited electronic states overlap over a wide energy range. The $^4\Pi_u$ state is substantially stabilized upon bending, where it becomes $^4B_1$, and is capable of predissociating lower-lying states. Dissociation of $CO_2^+$ has been shown[15] to proceed by predissociation of the $^2\Sigma g^+$ state

$$CO_2(^1\Sigma_g^+) + 19.1\ \text{eV} \rightarrow CO_2^+(^2\Sigma_g^+) \rightarrow O^+(^4S) + CO(^1\Sigma^+) \qquad (2)$$

Fluorescence from $^2\Sigma_g^+$ is not observed, and predissociation occurs from the ground vibrational state of $^2\Sigma_g^+$. Our results imply that the $^4\Pi_u$ surface is capable of predissociating $^2\Sigma_g^+$ in the Franck-Condon region of the ground vibrational state. It is furthermore possible to correlate the $^4\Pi_u$ $CO_2^+$ and $O^+$, CO asymptote symmetries with a $C_s$ reaction path. The observed reaction[16]

$$CO_2(^1\Sigma_g^+) + 19.47 \text{ eV} \rightarrow CO^+(^2\Sigma^+) + O(^3P) \quad (3)$$

is suggested by our results to proceed via a linear reaction path, again involving predissociation by the $^4\Pi_u$ surface. The reaction

$$C^+(^2P) + O_2(^3\Sigma_g^+) \rightarrow CO^+ + O \quad (4)$$

is reported to be fast. Our results favor the asymptotes $CO^+$ $(^2\Sigma^+)$, $O(^3P)$, since these connect adiabatically to the reagent states via the $CO_2^+(^4\Pi_u)$ surface. The set of reverse reactions

$$O^+(^4S) + CO(^1\Sigma^+) \rightarrow CO^+(^2\Sigma^+) + O(^3P) - .4 \text{ eV} \quad (5)$$

$$CO^+(^2\Sigma^+) + O(^3P) \rightarrow CO(^1\Sigma^+) + O^+(^4S) + .4 \text{ eV} \quad (6)$$

have been observed.[17-19] According to our results, the reagents of Reaction (5) would approach on the $^4A''$ $(^4\Pi_u)$ surface, to which they correlate in $C_s$ symmetry. Products would then be formed by population of the $^4A'(^4\Pi_u)$ surface. The exothermic Reaction (6) has been observed to be fast,[19] and could occur by the reverse of the process described for Reaction (5). However, there are necessary surface crossings in the asymptotic surfaces, and for this reason alone the reaction should be fast.

Negative Ion $CO_2^-$

The linear-bent correlation diagram for $CO_2^-$ is presented on Figure 3. As was found for $CO_2^+$, known and unknown excited electronic states overlap over a wide energy range. The $^4\Pi_g$, $^2\Phi_g$ and $^2\Pi_g$ can all be expected to predissociate the $^2\Sigma_u^+$ and $^2\Sigma_g^+$ states, and, in some cases, possibly the $^2B_1$ Renner split component of

$^2\Pi_u$. We predict that $CO_2^-(X^2A_1)$ is metastable, in agreement with other *ab initio* results,[10,11] and with experiment,[12] but in direct contradiction with semiempirical findings.[9] Our assignments of the excited states also differ from the semiempirical assignments. We find the $^2\Phi_g$ state to lie above $^2\Sigma_u^+$, whereas the semiempirical study finds just the opposite. As a consequence, our correlation diagram supports different predissociation and reaction mechanism possibilities from those that could be deduced from the semiempirical results.

We predict a vertical electron affinity of ∿-4 eV, which agrees with experimental estimates.[20] The adiabatic electron affinity is estimated to be ∿-1 eV on the basis of our results, in reasonable agreement with experiment.[21-24]

The overall features of the correlation diagram suggest that intersection of the ground state $CO_2/CO_2^-$ potential energy surfaces will be similar to the intersection of the isoelectronic $N_2O/N_2O^-$ potential surfaces which we describe in detail in a later section of this report. We therefore predict that the dissociative attachment

$$CO_2(X^1\Sigma_g{}^+) + e \rightarrow CO(X^1\Sigma^+) + O^-(^2P) \tag{7}$$

will yield vibrationally excited $CO(X^1\Sigma^+)$. This agrees with experimental suggestions.[25] The associative detachment

$$O^-(^2P) + CO(^1\Sigma^+) \rightarrow CO_2(^1\Sigma_g^+) + e \tag{8}$$

should also be overall similar to the corresponding $O^-$, $N_2$ detachment process. However, the electron affinities of $CO_2$ appear to be significantly larger than those of $N_2O$, and this may account for the fact that Reaction (8) is moderately fast,[27-30] whereas the corresponding $O^-$, $N_2$ detachment is slow.

## C. Valence States, Mixed Character States, and Rydberg States in Neutral $CO_2$

An interesting feature in the electronic spectra of $CO_2$ and other molecules is that the electronic states fall into three qualitatively different classes. The first class consists of valence states, whose spacial extents are similar to that of ground state $CO_2(X^1\Sigma_g^+)$. The second class consists of mixed character, or large states, whose spacial extents are much beyond the valence state region. Rydberg states make up the third class, viz. Those satisfying the Rydberg formula[6]

$$\Delta E_i = 13.605/[n^*(E)]^2 \quad \text{(units are eV)} \tag{9}$$

where

$$\Delta E_i = E(\text{Neutral State}) - E(\text{Parent Ion State}) \tag{10}$$

and $n^*(E)$ is the effective quantum number. In the case of mixed and Rydberg states, the character (spacial extent, validity of Equation (9)) is determined by a single outer occupied orbital.

We computed an accurate self-consistent-field (SCF) vertical spectrum for $CO_2$ in order to determine which of the states were valence, mixed character, or Rydberg states. All single electron excitations out of the four highest occupied molecular orbitals (MO's) into the five unoccupied MO's $2\pi_u$, $5\sigma_g$, $4\sigma_u$, $1\delta_g$ and $2\pi_g$ were included, giving a total of 60 electronic states. The energy levels are shown on Figure 4. Orbital energies, orbital second moments, and the second moment analog of Equation (10),

$$\Delta Q_i = Q(\text{Neutral State}) - Q(\text{Parent Ion State}) \qquad (11)$$

were computed. Effective quantum numbers for the mixed and Rydberg states were calculated from Equation(9), and from the hydrogenic formula

$$n^*(\bar{r}^2) = [0.5b_\ell + 0.5(b_\ell^2 + 1.6\bar{r}^2)^{\frac{1}{2}}]^{\frac{1}{2}} \qquad (12)$$

with

$$b_\ell = 0.6[\ell(\ell+1) - 1/3] \qquad (13)$$

The angular quantum numbers, $\ell$, could be determined without ambiguity from the character of the MO in question. The SCF computations give representations of five MO's ($2\pi_u$, $5\sigma_u$, $4\sigma_u$, $1\delta_g$ and $2\pi_g$) which are unoccupied in ground state $CO_2(X^1\Sigma_g{}^+)$. The $5\sigma_g$ is always a large, or mixed character MO, and hence each electronic state in which the $5\sigma_g$ is occupied is a mixed character state. This contradicts earlier, less accurate, *ab initio* findings.[7,8] The $4\sigma_u$, $1\delta_g$ and $2\pi_g$ are always Rydberg MO's, and thus electronic states in which one of these MO's is occupied are always Rydberg states. The $2\pi_u$ MO is fundamentally different, and can have either valence or Rydberg character. It has Rydberg character in the V-states $^1\Sigma_u^+$ and $^1\Sigma_g^+$, and otherwise has valence character.

The SCF and experimental Rydberg series are compared in Table 1. All experimental Rydberg levels with $n^* \lesssim 3$ have been included, since this is the range of $n^*$ we have considered theoretically. The agreement between theory and experiment is very good, and the symmetries of the electronic states corresponding to the observed series are here definitely assigned for the first time. However, none of the SCF Rydberg levels gives the experimentally observed

$n^* = 2.70$. Preliminary analysis suggests that the $6\sigma_g$ MO is involved, which we did not include in the present work.

To a good approximation, many Rydberg state characteristics depend only on the Rydberg MO. Average values for the Rydberg MO's are reported in Table 2. Each row of the table contains the average value for a given Rydberg MO. For example, the second entry in the first row is the average of all the $2\pi_g$ MO orbital energies we computed. Deviations about the averages are at worst a few percent, and usually smaller. Note that the two different theoretical ways of computing effective quantum numbers, $n^*(E)$ and $n^*(\bar{r}^2)$, are in close agreement.

D. <u>Vertical Spectrum Including Electron Correlation for Valence States of the Configuration $1\pi_g^3\ 2\pi_u^1$ in $CO_2$</u>

The configuration $1\pi_g^3\ 2\pi_u^1$ can be angular momentum coupled to form the electronic states ${}^{1,3}\Sigma_u^+$, ${}^{1,3}\Sigma_u^-$, ${}^{1,3}\Delta_u$. The V-state ${}^1\Sigma_u^+$ is Rydberg in character, and will not be considered here. By allowing valence and Rydberg character to mix, the remaining states were found to be valence states. Definitive experimental state assignments for these valence states have not been given, and previous theoretical treatments[7,8] of them have been of only modest accuracy. In the overall spirit of our theoretical project, namely, method calibration and evaluation, we have therefore performed several theoretical calculations of the electronic states in question which employ successively more accurate approximations, all of which are more accurate than the existing theoretical data. We first performed self-consistent-field (SCF) and multiconfiguration self-consistent-field calculations, followed by configuration interaction, (MCSCF/CI) with accurate (polarized) expansion sets. These differed markedly from the existing theoretical spectra, implying that the latter could only be accurate if cancellation of expansion set and correlation energy errors occurred. We next carried out equations-of-motion (EOM) calculations with accurate polarized expansion sets. The EOM calculations incorporate a more complete treatment of the correlation energy, and provide the most accurate theoretical spectrum currently available. We find for the EOM vertical excitation energies

$$
\begin{array}{lcl}
{}^3\Sigma_u^+ & : & 7.41 \text{ eV} \\
{}^3\Delta_u & : & 8.13 \text{ eV} \\
{}^3\Sigma_u^- & : & 8.45 \text{ eV} \\
{}^1\Sigma_u^- & : & 8.51 \text{ eV} \\
{}^1\Delta_u & : & 8.51 \text{ eV}
\end{array}
$$

Interestingly enough, these values are fortuitously close to the existing limited accuracy theoretical spectra.

### E. Future Goals

Potential energy surface priorities begin with the ground state surface of neutral $CO_2$. More information exists[31-39] for this potential surface than for any others in the molecules $CO_2$/ $CO_2^+$/ $CO_2^-$. We will exploit this to simultaneously assess our own surfaces and several ways of computing triatomic force constants. Armed with a suitably calibrated method, we will then probe the ground state surface of neutral $CO_2$ to whatever extent is necessary. Proper dissociation will be especially emphasized. Beyond this we will investigate $CO_2^+$ potential surfaces, which are so important in ionospheric ion-molecule reactions. An investigation of the intersection of the $CO_2/CO_2^-$ ground state potential surfaces is also envisioned.

Investigation of neutral $CO_2$ excited states will also continue. Locating the lowest $^1\Delta_u$ and $^1\Pi_g$ states relative to one another appears to be needed for understanding possible reaction mechanisms. Both are optically forbidden states, and hence are difficult to probe experimentally. Our current theoretical results imply that the states are nearly degenerate. The Rydberg character of the excited states as a function of geometry is likewise of interest. If the Rydberg character changes with the geometry, the state in question may not behave like its parent ion state, and hence its role in chemical reactions cannot be reliably predicted based on ion states.

Very little is known about the ionization of inner electrons in $CO_2$, and also of shake-up ionization. The $^4\Sigma_g^-$ ion state may have predissociation capabilities similar to the $^4\Pi_u$ ion state that we discussed in this report. The location of the $^4\Sigma_g^-$ state, and of other unknown $CO_2^+$ states, will therefore be determined.

There may be low-lying states of $CO_2^-$ which lie in the energy range that we reported here. Using methods similar to those we describe for $O_3^-$ elsewhere in this document, a closer scan of possible excited states will be undertaken. Ultimately, a re-analysis of the experiments as given in Reference 9 is required with reliable *ab initio* curves.

## REFERENCES


1. R. S. Mulliken, Rev. Mod. Phys. **14**, 204 (1942).

2. A. D. Walsh, J. Chem. Soc. 2226 (1953).

3. R. N. Dixon, Disc. Faraday Soc. **35**, 105 (1963).

4. R. N. Dixon, Proc. Roy. Soc. (London) **A275**, 431 (1963).

5. D. W. Turner, A. D. Baker, and C. R. Brundle, "Molecular Photoelectron Spectroscopy," (John Wiley, New York, 1970).

6. A. B. F. Duncan, "Rydberg Series in Atoms and Molecules," (Academic Press, New York, 1971).

7. C. W. McCurdy, Jr. and V. McKoy, J. Chem. Phys. **61**, 2820 (1974).

8. N. W. Winter, C. F. Bender and W. A. Goddard III, Chem. Phys. Lett. **20**, 489 (1973).

9. C. R. Claydon, G. A. Segal, and H. S. Taylor, J. Chem. Phys. **52**, 3387 (1970).

10. M. Krauss and D. Neumann, Chem. Phys. Lett. **14**, 26 (1972).

11. J. Pacansky, V. Wahlgren, and P. S. Bagus, J. Chem. Phys. **62**, 2740 (1975).

12. C. D. Cooper and R. N. Compton, Chem. Phys. Lett. **14**, 29 (1972).

13. M. A. A. Clyne and B. A. Thrush, Proc. Roy. Soc. (London) **A269**, 404 (1962).

14. M. C. Lin and S. H. Bauer, J. Chem. Phys. **50**, 3377 (1969).

15. J. H. D. Eland, Int. J. Mass Spectrom. Ion Phys. **9**, 397 (1973).

16. K. E. McCulloh, J. Chem. Phys. **59**, 4250 (1973).

17. E. Murad, J. Chem. Phys. **58**, 4374 (1973).

18. F. C. Fehsenfeld, D. L. Albritton, Y. A. Bush, D. G. Fournier, T. R. Grovers, and J. Fournier, J. Chem. Phys. **61**, 2150 (1974).

19. F. C. Fehsenfeld and E. E. Ferguson, J. Chem. Phys. **56**, 3066 (1972).

20. Experimental results are summarized in Reference 9.

21. T. O. Tiernan and R. P. Clow, Adv. Mass Spec. **6**, 295 (1974).

REFERENCES, Cont'd


22. R. A. Holroyd, T. E. Gangwer and A. O. Allen, Chem. Phys. Lett. **31**, 520 (1975).

23. R. N. Compton, P. W. Reinhardt, and C. D. Cooper, J. Chem. Phys. **63**, 3821 (1975).

24. R. P. Clow and T. O. Tiernan, J. Chem. Phys., to be published.

25. P. J. Chantry, J. Chem. Phys. **57**, 3180 (1972).

26. F. C. Fehsenfeld, E. E. Ferguson, and A. L. Schmeltekopf, J. Chem. Phys. **45**, 1844 (1966).

27. J. L. Moruzzi, J. W. Ekin, Jr., and A. V. Phelps, J. Chem. Phys. **48**, 3070 (1968).

28. E. E. Ferguson, Acct. Chem. Res. **3**, 402 (1970).

29. M. McFarland, D. L. Albritten, F. C. Fehsenfeld, E. E. Ferguson, and A. L. Schmeltekopf, J. Chem. Phys. **59**, 6629 (1973).

30. A. E. Roche and C. C. Goodyear, J. Phys. **B2**, 191 (1969).

31. A. B. Anderson, J. Chem. Phys. **57**, 4143 (1972).

32. M. A. Pariseau, I. Suzuki, and J. Overend, J. Chem. Phys. **42**, 2335 (1965).

33. I Suzuki, J. Mol. Spectry, **25**, 479 (1968).

34. R. G. Parr and J. E. Brown, J. Chem. Phys. **49**, 4849 (1968).

35. D. F. Smith, Jr., and J. Overend, J. Chem. Phys. **53**, 2411 (1970).

36. J. E. Brown and R. G. Parr, J. Chem. Phys. **54**, 3429 (1971).

37. A. B. Anderson, J. Chem. Phys. **56**, 4228 (1972).

38. A. B. Anderson, J. Mol. Spectry. **44**, 411 (1972).

39. M. Vucelič, Y. Öhrn, and J. R. Sabin, J. Chem. Phys. **59**, 3003 (1973)

Table 1. Rydberg states and MO configurations for $CO_2$. The experimental results were taken from Ref. 6, where references to the original work can be found.

| Ion State | Rydberg State | MO Configuration | $\delta$[a] Expt. | $\delta$[a] SCF | $n^*$ Expt. | $n^*$ SCF | $\Delta E_i$ (eV) Expt. | $\Delta E_i$ (eV) SCF |
|---|---|---|---|---|---|---|---|---|
| | $^1\Sigma_u^+$ | $1\pi_g^{-1}p_\pi$ | 0.65 | 0.65 | 2.35 | 2.35 | 2.46 | 2.46 |
| $X^2\Pi_g$ | $^{1,3}\Pi_u$ | $1\pi_g^{-1}p_\sigma$ | 0.57 | 0.53 | 2.43 | 2.47 | 2.30 | 2.23 |
| | $^{1,3}\Sigma_g^\pm$, $^{1,3}\Delta_g$ | $1\pi_g^{-1}d_\pi$ | 0.97 | 0.96 | 3.03 | 3.04 | 1.48 | 1.47 |
| $A^2\Pi_u$ | $^{1,3}\Phi_u$, $^{1,3}\Pi_u$ | $1\pi_u^{-1}d_\delta$ | 0.093 | 0.05 | 2.907 | 2.95 | 1.61 | 1.56 |
| $B^2\Sigma_u^+$ | $^{1,3}\Pi_u$ | $3\sigma_u^{-1}d_\pi$ | 0.90 | 0.94 | 3.10 | 3.06 | 1.42 | 1.45 |
| | | | 0.30 | | 2.70 | | 1.87 | |
| $C^2\Sigma_g^+$ | $^{1,3}\Delta_g$ | $4\sigma_g^{-1}d_\delta$ | 0.05 | 0.00 | 2.95 | 3.00 | 1.56 | 1.51 |

[a] Quantum defect.

Table 2. Average Rydberg state expectation values.

| MO | $\Delta E_i$ [a] | $-\varepsilon$ [a,b] | $\overline{r^2}$ [c,d] | $\overline{z^2}$ [c,d] | $\overline{x^2}$ [c,d] | $\Delta\Omega_i$ [e] | $q$ [e,f] | n*(E) | n*($\bar{r}$ |
|---|---|---|---|---|---|---|---|---|---|
| $2\pi_g(d_\pi)$ | 1.45 | 1.45 | 146.3 | 62.7 | 41.8 | -28.0 | -28.2 | 3.07 | 3.09 |
| $1\delta_g(d_\delta)$ | 1.53 | 1.53 | 120.0 | 17.2 | 51.4 | 46.0 | 46.1 | 2.98 | 2.98 |
| $4\sigma_u(p_\sigma)$ | 2.23 | 2.25 | 84.0 | 50.1 | 17.0 | -43.8 | -44.6 | 2.47 | 2.51 |
| $2\pi_u(p_\pi)$ | 2.46 | 2.49 | 66.3 | 13.2 | 26.6 | 17.8 | 18.0 | 2.35 | 2.38 |

[a] Units are eV.

[b] $\varepsilon$ = orbital energy of Rydberg MO.

[c] Rydberg MO expectation value, origin at C and bonds along z-axis.

[d] Units are $a_o^2$, $a_o$ = Bohr radius.

[e] Units are esu-cm$^2$ x $10^{26}$.

[f] Rydberg MO second moment.

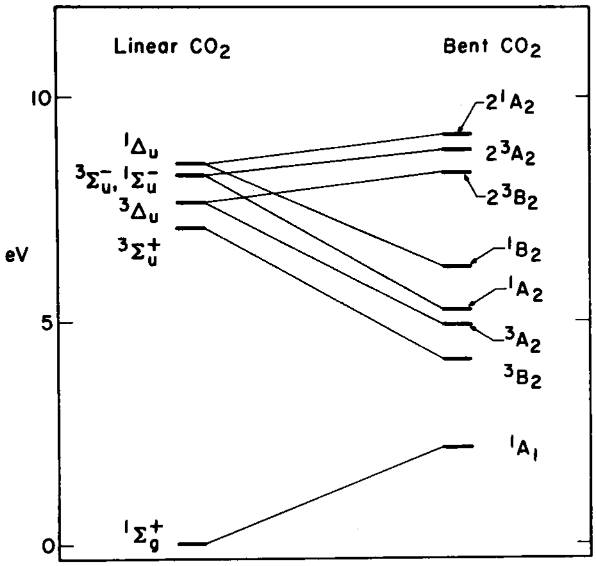


Fig. 1.

SCF State Correlation Diagram for Linear and Bent $CO_2$. The Energy Zero is $CO_2(^1\Sigma_g^+)$.

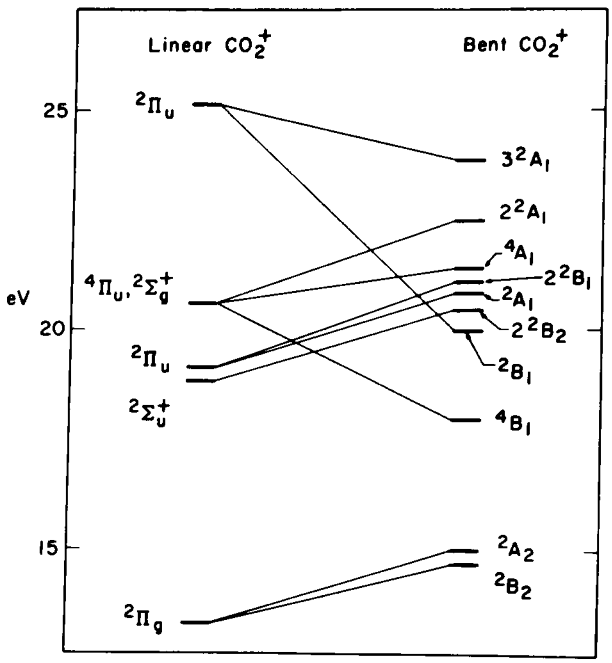


Fig. 2.

SCF State Correlation Diagram for Linear and Bent $CO_2^+$. The Energy Zero is $CO_2(^1\Sigma_g^+)$.

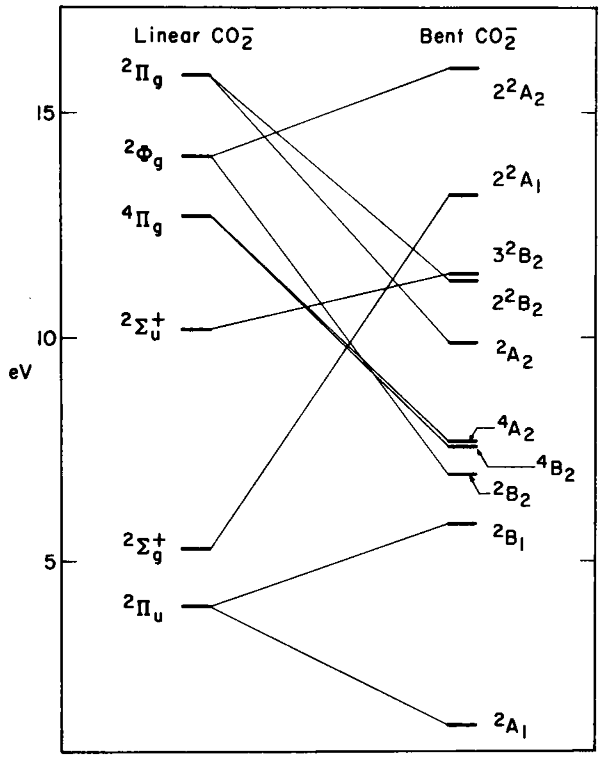


Fig. 3.

SCF State Correlation Diagram for Linear and Bent $CO_2^-$. The Energy Zero is $CO_2(^1\Sigma_g^+)$.

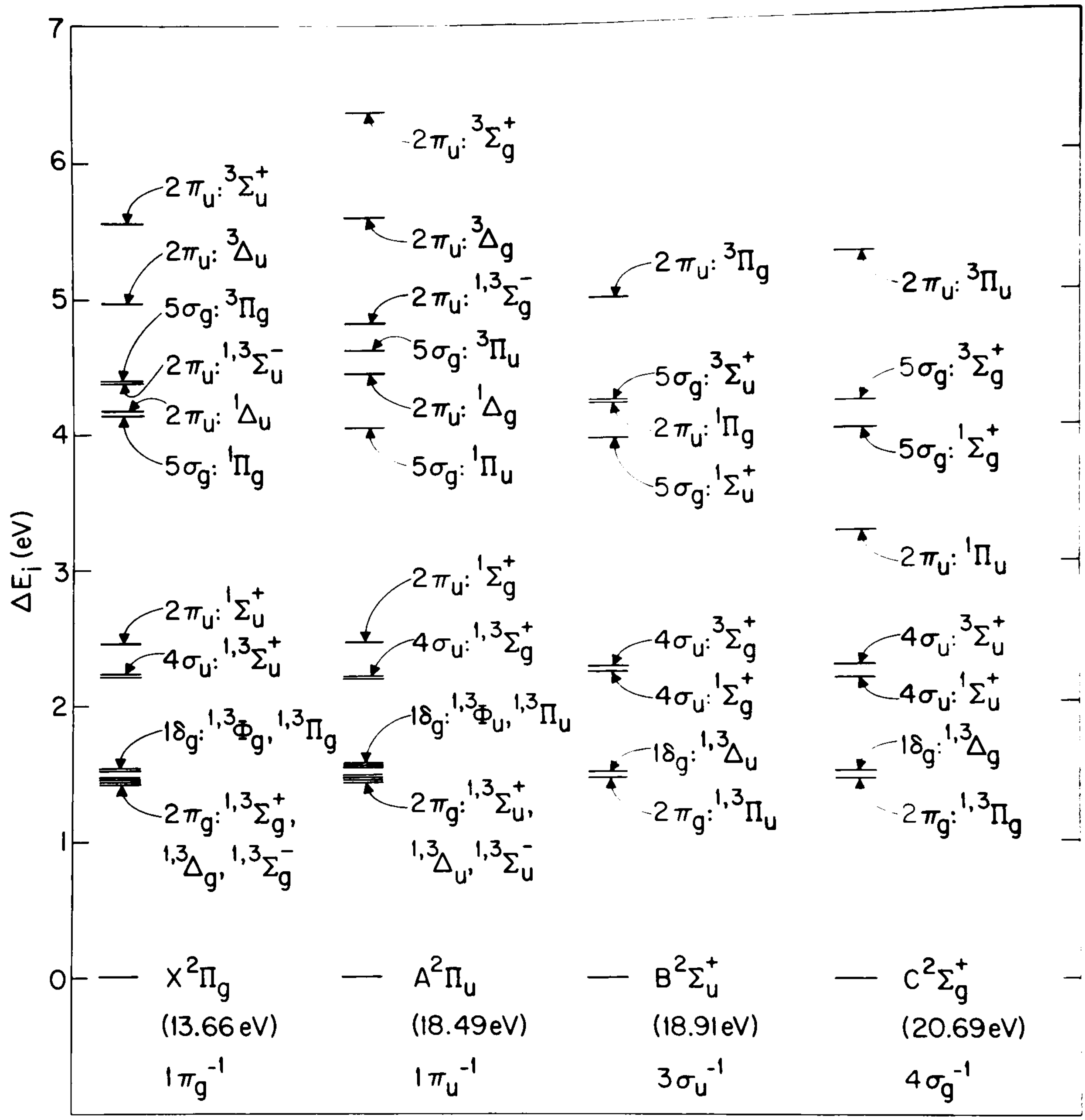


Fig. 4.

Vertical SCF Spectrum of Neutral $CO_2$ Relative to the Four Lowest States of $CO_2^+$.

# OZONE AND ITS IONS

## A. Introduction

Experimentally, there are two states connected by dipole-allowed transitions to the ground $^1A_1$ state of ozone.[1,2] The Chappuis band is assigned to the $^1B_1$ state, and the Hartley band is assigned to the $^1B_2$ state. In addition, the Huggins band has been attributed to the non-vertical part of the $^1B_2 \leftarrow {}^1A_1$ transition, while the Wulf band has been assigned to the dipole-forbidden $^1A_2 \leftarrow {}^1A_1$ transition. Recent electron energy loss spectroscopy has been used to detect the existence of at least one bound low-lying triplet state.[3] The electronic spectra beyond the Hartley band has been reported,[1] including the electron energy loss spectra for an energy loss range of 1-30 eV.[4] A variety of *ab initio* methods (self-consistent field, generalized valence-bond, and configuration interaction) have been used to compute the electronic spectra of ozone.[5-8] Three states were found to be bound and a total of eight states had excitation energies lower than 6 eV.[8]

The spectra of $O_3^+$ has been studied by the high resolution photoelectron spectroscopy of ozone.[9-11] Three bands, between 12 and 14 eV, with accompanying vibrational structure were identified and attributed to ionization from the $6a_1$, $1a_2$ and $4b_2$ orbitals. Two studies[10-11] assigned the order of the ion states as $X^2A_1$, $A^2A_2$, $B^2B_2$, whereas the third study[9] assigned the ordering $X^2A_1$, $A^2B_2$, $B^2A_2$. Koopmans' Theorem incorrectly predicts the ground state of $O_3^+$ to be $^2A_2$, with the discrepancy arising not from differential orbital relaxation effects but from differences in the correlation energies of the ionic states.[12] Multi-configuration self-consistent field/configuration interaction calculations[13] support the assignment of the first two excited states as $A^2A_2$, $B^2B_2$ , whereas the more extensive generalized valence-bond/configuration interaction calculations[8] yields an ordering of $A^2B_2$, $B^2A_2$.The photoelectron spectra all show additional broad bands at higher energies corresponding to ionization from inner orbitals followed by shake-up processes, with all three studies differing on the number and orbital-state assignments of such bands. The *ab initio* calculations also disagree with each other (as well as with experiment) on the assignment of the higher states of $O_3^+$.

Matrix isolation spectroscopy has been used to study the vibrational and electronic spectroscopy of the $O_3^-$ ozonide ion.[14,15] In addition, the electronic absorption and resonance Raman spectra of $O_3^-$ have been studied by means of γ-irradiated spectra of alkali-metal halates.[16,17] Only one electronic transition is observed for $O_3^-$ and is assigned as $^2A_2 \leftarrow X^2B_1$.[14] A variety of experimental techniques (charge transfer reactions,[18,19] lattice energy calculations,[20] collisional ionization,[21] drift-tube photodetachment[22,23]) as well as an *ab initio* configuration interaction calculation[24] have been used to determine the electron affinity of ozone, and the consensus of results indicates a value of ∿ 2.0-2.1 eV.

B. OZONE

*Ab initio* self-consistent field (SCF) and multi-configuration self-consistent field/configuration interaction (MCSCF/CI) calculations were performed on the lowest singlet and triplet states of $O_3$ at a single geometry corresponding to the experimental equilibrium geometry of the ground $1^1A_1$ state ($R_{O-O}$ = 1.2717Å = 2.403 $a_0$, θ =

116.78°)[25]. Based on earlier SCF calculations,[26] the manifold of states of a given symmetry which result from various occupancies of the $6a_1$, $4b_2$, $2b_1$ and $1a_2$ valence orbitals are all quite close in energy. Thus a priori selection of the dominant Hartree-Fock configuration for a given state is not possible, and it is necessary to compute energies for several configurations of the same symmetry in order to determine the lowest one.

The computed SCF and MCSCF/CI vertical excitation energies for the valence states of $O_3$ are given in Table I. An examination of the SCF results reveals that the $^3B_2$ state is incorrectly predicted to be the ground state at this level of computation; this incorrect state ordering was also found in other theoretical calculations.[8] Moreover, there is a reordering of some of the other excited states. The including of correlation energy results in a correct ordering of the $^1A_1$ and $^3B_2$ states. The present MCSCF/CI excitation energies are within the reported experimental range of energies for the observed transitions. It should be noted that the order and position of the electronic states of $O_3$ can be expected to vary significantly with geometry, even to the extent of inverting the ground and excited states.[8]

C. POSITIVE ION $O_3^+$

SCF and MCSCF/CI calculations were performed on the lowest doublet and quartet states of $O_3^+$ at the experimental equilibrium geometry of the $X^1A_1$ state of $O_3$. The results of the vertical excitation energies are given in Table II. On theoretical grounds we expect $O_3^+$ to have an energy surface behavior comparable to $NO_2$. Although Koopmans' Theorem predicts the ground state of $O_3^+$ to be $^2A_2$, the experimental ground state of the isoelectronic $NO_2$ molecule is $^2A_1$.[1] Once again the SCF calculations do not yield the correct ground, as also found in other theoretical works.[12,13] Including correlation energy results in the correct ground state and shows the first excited state to be $^2B_2$.

The computed three lowest ionization potentials of $O_3$ are given in Table III, and are compared with experimental results. The MCSCF/CI values are all in error by 1.5-1.8 eV. We presently attribute the large errors in our calculated ionization potentials to restrictions in the present level of our computational method.

D. NEGATIVE ION $O_3^-$

SCF and MCSCF/CI calculations were performed on the lowest doublet and quartet states of $O_3^-$ at the experimental equilibrium geometry of the $X^1A_1$ state of $O_3$. Previous experimental[14] and theoretical[24] studies estimate the equilibrium geometry of the $X^2B_1$ state of $O_3^-$ to be near that of the ground state of the neutral molecule. The computed vertical excitation energies are given in Table IV. In contrast to what was found for the $O_3$ and $O_3^+$ systems, SCF calculations are sufficient for a correct prediction of the ground state of $O_3^-$. The results for the quartet vertical excitation energies must be viewed with caution since these states are unstable in the SCF approximation. The MCSCF/CI calculation is in error by $\sim$ 1 eV with the one experimentally observed transition, $^2A_2 \leftarrow X^2B_1$. The present results would seem to better support an assignment of $^2A_1 \leftarrow X^2B_1$, but deficiencies in the computations preclude any reassignments at the present time. It should also be noted that the electronic spectra of $O_3^-$ were studied in an argon matrix, not in the gas phase; thus the value of the measured transition energy may be significantly affected by environmental interactions. The computed SCF electron affinity exceeds the experimental values by $\sim$ 0.3 eV, while the use of correlated wavefunctions, in their present level, fails to bind the electron to ozone.

## E. FUTURE GOALS

Future work will deal with the extension of present levels and types of computational procedures in order to more accurately calculate energy quantities, especially energy differences between systems having different numbers of electrons (e.g., ionization potentials, electron affinity). A primary objective of this work will be the assignment of the high energy bands in the photoelectron spectra of $O_3$, as well as the prediction of some yet unobserved transitions in the $O_3^-$ ozonide ion.

We also propose to compute portions of the potential energy surface of the $X^1A_1$ state of ozone, with the principal emphasis in the well region to compute bound vibrational levels and spectroscopic constants. The vibrational deactivation of $O_2(^3\Sigma_g^-)$ by $O(^3P)$,[27-29] and the three body recombination process,

$$O(^3P) + O_2(^3\Sigma_g^-) + M \rightarrow O_3(X^1A_1) + M,^{30-31}$$

are additional topics of interest involving the ground state potential surface.

REFERENCES


1. G. Herzberg, *Molecular Spectra and Molecular Structure* (Van Nostrand, Princeton, 1967), Vol. 3.

2. M. Griggs, J. Chem. Phys. **49**, 857 (1968).

3. N. Swanson and R. J. Celotta, Phys. Rev. Lett. **35**, 783 (1975).

4. R. J. Celotta, S. R. Mielczarek, and C. E. Kuyatt, Chem. Phys. Lett. **24**, 428 (1974).

5. P. J. Hay and W. A. Goddard III, Chem. Phys. Lett. **14** 46 (1972).

6. W. A. Goddard III, T. H. Dunning, Jr., W. J. Hunt, and P. J. Hay, Accts. Chem. Res. **6**, 368 (1973).

7. P. J. Hay, T. H. Dunning, Jr., and W. A. Goddard III, Chem. Phys. Lett. **23**, 457 (1973).

8. P. J. Hay, T. H. Dunning, Jr., and W. A. Goddard III, J. Chem. Phys. **62**, 3912 (1975).

9. J. M. Dyke, L. Golob, N. Jonathan, A. Morris, and M. Okuda, J. Chem. Soc. Faraday Trans. II, **70**, 1828 (1974).

10. D. C. Frost, S. T. Lee, and C. A. McDowell, Chem. Phys. Lett. **24**, 149 (1974).

11. C. R. Brundle, Chem. Phys. Lett. **26**, 25 (1974).

12. I. H. Hillier and J. Kendrick, J. Chem. Soc. Faraday Trans. II. **71**, 1906 (1975).

13. H. Basch, J. Amer. Chem. Soc. **97**, 6047 (1975).

14. M. E. Jacox and D. E. Milligan, J. Mol. Spectry. **43**, 148 (1972).

15. L. Andrews, J. Chem. Phys. **63**, 4465 (1975).

16. J. B. Bates and J. C. Pigg, J. Chem. Phys. **62**, 4227 (1975).

17. G. E. Boyd and L. C. Brown, J. Phys. Chem. **74**, 3490 (1970).

18. J. Berkowitz, W. A. Chupka, and D. Gutman, J. Chem. Phys. **55**, 2733 (1971).

19. E. E. Ferguson, Can. J. Chem. **47**, 1815 (1969).

20. R. H. Wood and L. A. D'Orazio, J. Phys. Chem. **69**, 2562 (1965).

REFERENCES

21. E. W. Rothe, S. Y. Tang, and G. P. Reck, J. Chem. Phys. **62**, 3829 (1975).

22. R. Byerly, Jr., and E. C. Beaty, J. Geophys. Res. **76**, 4596 (1971).

23. S. F. Wong, T. V. Vorburger, and S. B. Woo, Phys. Rev. **A5**, 2598 (1972).

24. M. M. Heaton, A. Pipano, and J. J. Kaufman, Int. J. Quantum Chem. **S6**, 181 (1972).

25. T. Tanaka and Y. Morino, J. Mol. Spectry. **33**, 538 (1970).

26. S. D. Peyerimhoff and R. J. Buenker, J. Chem. Phys. **47**, 1953 (1967).

27. J. H. Kiefer and R. W. Lutz, Symp. Combust. 11th, Berkeley, California, 1966, 67 (1967).

28. H. Webster and E. J. Blair, J. Chem. Phys. **56**, 6104 (1972).

29. E. L. Breig, J. Chem. Phys. **51**, 4539 (1969).

30. H. Johnston, NSRDS 20 (U.S.) (1968).

31. R. E. Huie, J. T. Herron, and D. D. David, J. Phys. Chem. **76**, 2653 (1972).

Table I. Vertical excitation energies for $O_3$, $R_{0-0} = 2.403\ a_o$, $\theta = 116.8°$.[a]

| State | SCF | MCSCF/CI | Expt.[b,c] |
|---|---|---|---|
| $X^1A_1$ | 1.7 | 0.0 | 0.0 |
| $1^1A_2$ | 3.2 | 2.1 | 1.2-2.0 |
| $1^1B_1$ | 3.5 | 2.3 | 2.0-2.3 |
| $1^1B_2$ | 5.9 | 5.4 | 4.1-5.7 |
| $1^3A_1$ | 7.5 | 8.0 | |
| $1^3A_2$ | 2.8 | 2.0 | |
| $1^3B_1$ | 2.7 | 1.9 | |
| $1^3B_2$ | 0.0 | 1.6 | |

[a] All energies in electron volts.

[b] G. Herzberg, *Molecular Spectra and Molecular Structure*, (Van Nostrand, 1967), Vol. 3.

[c] M. Griggs, J. Chem. Phys. 49, 857 (1968).

Table II. Vertical excitation energies for $O_3^+$, $R_{O-O} = 2.403\ a_o$, $\theta = 116.8°$.[a]

| State | SCF | MCSCF/CI |
|---|---|---|
| $X^2A_1$ | 3.8 | 0.0 |
| $1^2A_2$ | 0.7 | 0.5 |
| $1^2B_1$ | 5.6 | 3.2 |
| $1^2B_2$ | 3.8 | 0.1 |
| $1^4A_1$ | 1.7 | 1.9 |
| $1^4A_2$ | 0.0 | 2.7 |
| $1^4B_1$ | 4.9 | 4.9 |
| $1^4B_2$ | 1.0 | 1.4 |

[a]All energies in electron volts.

Table III. Vertical ionization potentials of $O_3$, $R_{0-0} = 2.403\ a_o$, $\theta = 116.8°$.[a]

| Orbital | State | SCF | MCSCF/CI | Expt.[b,c,d] |
|---|---|---|---|---|
| $6a_1$ | $X^2A_1$ | 13.8 | 11.3 | 12.75 |
| $4b_2$ | $1^2B_2$ | 13.8 | 11.4 | 13.03 |
| $1a_2$[e] | $1^2A_2$ | 10.8 | 11.8 | 13.57 |

[a]All energies in electron volts.

[b]J. M. Dyke, L. Golob, N. Jonathan, A. Morris, and M. Okuda, J. Chem. Soc. Faraday Trans. II, **70**, 1828 (1974).

[c]D. C. Frost, S. T. Lee, and C. A. McDowell, Chem. Phys. Lett. **24**, 149 (1974).

[d]C. R. Brundle, Chem. Phys. Lett. **26**, 25 (1974).

[e]The dominant HF configuration, as used in the SCF calculation, for the $^2A_2$ state does not correspond to simple ionization from the $1a_2$ orbital, but rather to an ionization plus shake-up process.

Table IV. Vertical excitation energies for $O_3^-$, $R_{0-0}$ = 2.403 $a_o$, $\theta$ = 116.8°.[a]

| State | SCF | MCSCF/CI | Expt.[b] |
|---|---|---|---|
| $X^2B_1$[c] | 0.0(2.4) | 0.0(-0.5) | 0.0(1.47-2.1)[d-j] |
| $1^2A_1$ | 2.6 | 2.7 | |
| $1^2A_2$ | 4.2 | 3.7 | 2.8 |
| $1^2B_2$ | 2.9 | 2.9 | |
| $1^4A_1$ | 10.1 | 10.8 | |
| $1^4A_2$ | 9.0 | 8.3 | |
| $1^4B_1$ | 9.3 | 8.3 | |
| $1^4B_2$ | 7.3 | 8.3 | |

[a]All energies in electron volts.

[b]M. E. Jacox and D. E. Milligan, J. Mol. Spectry. **43**, 148 (1972).

[c]Number in parentheses is the electron affinity.

[d]J. Berkowitz, W. A. Chupka, and D. Gutman, J. Chem. Phys. **55**, 2733 (1971).

[e]E. E. Ferguson, Can. J. Chem. **47**, 1815 (1969).

[f]R. H. Wood and L. A. D'Orazio, J. Phys. Chem. **69**, 2562 (1965).

[g]E. W. Rothe, S. Y. Tang, and G. P. Reck, J. Chem. Phys. **62**, 3829 (1975).

[h]R. Byerly, Jr., and E. C. Beaty, J. Geophys. Res. **76**, 4596 (1971).

[i]S. F. Wong, T. V. Vorburger, and S. B. Woo, Phys. Rev. **A5**, 2598 (1972).

[j]M.M. Heaton, A. Pipano, and J.J. Kaufman, Int. J. Quantum Chem. **S6**, 181 (1972).

# NITROUS OXIDE AND ITS NEGATIVE ION

## A. Introduction

The $N_2O$, $N_2O^-$ molecules are isoelectronic with the systems $CO_2$, $CO_2^-$, respectively, and the Walsh-Mulliken rules[1,2] predict that linear and bent geometries play important roles in $N_2O$, $N_2O^-$ chemistry. The ground state $N_2O/N_2O^-$ prediction is that the minimum geometry of $N_2O$ is linear, and the minimum geometry of ground state $N_2O^-$ is bent. As was the case in the $CO_2$, $CO_2^-$ molecules, the potential energy surfaces intersect, with the ground state potential energy surface of $N_2O$ lying lowest for geometries near the linear equilibrium geometry of $N_2O$, and with the ground state potential energy surface of $N_2O^-$ lying lowest near the bent equilibrium geometry of $N_2O^-$. The details of these surfaces and their intersection bear directly on the possible ionospheric associative detachment reaction

$$O^-(^2P) + N_2(X^1\Sigma_g^+) \rightarrow N_2O(X^1\Sigma^+) + e + 0.21 \text{ eV} \qquad (1)$$

which has not been observed in laboratory experiments conducted at 300K. A low thermal rate constant has been assigned to Reaction (1) by several experimenters,[3-6] and conflicting reports exist[6,7] concerning reactivity above 0.3 eV relative collision energy (ground vibrational state $N_2$).

The low thermal rate constant for the exothermic Reaction (1) suggests that substantial barriers are involved in the intersection of the $N_2O$ and $N_2O^-$ potential energy surfaces, and that vibrationall excited reagent $N_2$ may appreciably enhance the reaction. Since vibrationally excited $N_2$ is common in the ionosphere, the characterization of the $N_2O$ and $N_2O^-$ potential surfaces, needed to predict the effects of vibrationally hot reagent $N_2$ on the rate of Reaction (1), warrants detailed investigation.

### B. The Ground State $N_2O$ and $N_2O^-$ Potential Energy Surfaces

Thermodynamic cycles can be constructed which express the adiabatic electron affinity of $N_2O$, $EA(N_2O)$, and the dissociation energy of the N-$NO^-$ bond in $N_2O^-$, $D(N\text{-}NO^-)$, in terms of known thermodynamic quantities:

$$EA(N_2O) = EA(O) + D(N_2\text{-}O^-) - D(N_2\text{-}O) \tag{2a}$$

$$D(N\text{-}NO^-) = EA(N_2O) + D(N\text{-}NO) - EA(NO) \tag{2b}$$

The values used are shown in Table 1, together with the resulting $EA(N_2O)$ and $D(N\text{-}NO^-)$ values.

*Ab initio* self-consistent-field (SCF) and multiconfiguration self-consistent-field, followed by configuration interaction (MCSCF/CI), wavefunction calculations were performed to determine the potential energy surfaces for $N_2O$ and $N_2O^-$. Equilibrium geometries and harmonic force constants and vibrational frequencies are shown in Table 2. It follows from these results that the shapes of the $N_2O$ and $N_2O^-$ potential energy surfaces should be reliably determined near their respective minima.

*Ab initio* bending and stretching potentials can be used to estimate the energy required to change the geometry of $N_2O^-$ from its equilibrium value to that of equilibrium $N_2O$. The computed values are listed in Table 3. The predicted barrier, 2.5 eV, is significantly higher than the exothermicity of Reaction (1), in support of a low thermal rate constant.

The intersection locus of the ground state $N_2O^-$ and $N_2O$ potential energy surfaces can be determined by fitting the *ab initio* $N_2O$ and $N_2O^-$ potential energy points with a functional form. It was found that a two-dimensional anharmonic Morse potential form was sufficient, in which one bondlength is treated parametrically. The anharmonicity is essential for close reproduction of the *ab initio* $N_2O$ vertical electron affinity. The minimum energy of intersection between the $N_2O$ and $N_2O^-$ potential surfaces is found to be $\sim$0.66 eV above the potential energy of equilibrium geometry $N_2O$. The geometry at the minimum energy of intersection is

$$R_{NO} = 1.28\text{Å} \tag{3a}$$

$$R_{NN} = 1.18\text{Å} \tag{3b}$$

$$\sphericalangle(\text{NNO}) = 155° \tag{3c}$$

The associative detachment threshold for Reaction (1)is obtained from the minimum energy intersection by adding the zero point energy of the minimum intersection energy complex and subtracting 1) the asymptotic $N_2 + O^-$ energy obtained from the anharmonic Morse form, and 2) the zero point energy of $N_2$. The predicted threshold for Reaction (1) is

$$E_a(\text{Rxn } 1) = 0.21 \text{ eV} \tag{4}$$

This activation energy is less than the energy necessary to excite reagent $N_2$ to the first excited vibrational state (0.29 eV). Furthermore, the $R_{NN}$ of Equation (3b) is greater by 0.04 Å than the classical anharmonic turning point for vibrationally cold $N_2$(1.146Å) and almost equal to the outer turning point for $N_2$ in its first excited vibrational state (1.185Å). Thus, the rate of Reaction (1) will probably not be enhanced by translational excitation of vibrationally cold $N_2$, but may be strongly enhanced by vibrational excitation of reagent $N_2$, with or without translational excitation.

The $N_2O$ and $N_2O^-$ potential energy surface intersection also provides information for the dissociative attachment threshold

$$N_2O(X^1\Sigma^+) + e \rightarrow N_2(X^1\Sigma_g^+) + O^-(^2P) - .21 \text{ eV} \qquad (5)$$

The electron detachment threshold for Reaction (5) is obtained from the minimum energy intersection by adding the zero point energy of the minimum intersection energy complex, and subtracting 1) the $N_2O$ equilibrium potential energy, and 2) the zero point energy of $N_2O$. The result is

$$Ea(Rxn(5)) = 0.40 \text{ eV} \qquad (6)$$

which is in good agreement with the experimental estimate of 0.45 eV.[8] Since the minimum intersection occurs with extended bondlengths relative to equilibrium $N_2O$, and at an angle about 25° away from linearity, it is very likely that the electron detachment described by Reaction (4) will be facilitated by excitation of the $N_2O$ bending and symmetric stretch modes.

The vertical electron affinity, or resonance energy, for $N_2O(^1\Sigma^+)$ can be reliably obtained from the previously computed adiabatic electron affinity by adding the zero point energy of $N_2O^-$, and subtracting 1) the zero point energy of $N_2O^-(^2\Pi)$, which is estimated to be the same as the $N_2$ zero point energy, 2) the barrier to bending, and 3) the barrier to contraction of the bondlengths. A vertical electron affinity of -2.23 eV results, which is in good agreement with broad experimental electron scattering peaks.[9]

### C. Conclusions

The ground state potential energy surface of $N_2O^-$ is stable in its equilibrium region to both associative detachment (Reaction (1)) and dissociation. The features of the ground state $N_2O/N_2O^-$ potential surfaces described in this report show why this is so. Associative detachment is immeasurably slow for reagent thermal $N_2$ because there is a barrier of $\sim$0.2 eV which the reagents must overcome to reach the minimum intersection energy of the $N_2O/N_2O^-$ surfaces. Moreover, the minimum intersection occurs at $R_{NN}$ bondlengths greater than the equilibrium $N_2$ bondlength, which suggests that vibrationally hot $N_2$ will be needed to effectively enhance reaction.

The dissociative attachment process (Reaction (5)) is likewise described by the $N_2O/N_2O^-$ potential surfaces. The $N_2O$ molecule must be vibrationally excited in order to reach the minimum energy of intersection of the $N_2O/N_2O^-$ surfaces. This requires at least the absorption of several bending vibrational quanta. Here, however, the threshold energy (0.4 eV) is sufficient to populate these levels. Since the minimum intersection energy involves slightly longer $R_{NN}$ and $R_{NO}$ than occur in $N_2O$, it is likely that the excitation of stretching vibrational quanta will further enhance reaction.

Our results also provide a vertical electron affinity of -2.23 eV for $N_2O(^1\Sigma^+)$. This value is thought to be reliable, since it was obtained with a method which does not involve a nonvariational determination directly.

D. Future Goals

There is evidence from experimental[10,11] and theoretical[12,13] studies that a major source of $N_2$ vibrational temperature in the upper atmosphere is its $E \rightarrow V,R,T$ energy transfer reaction with $O(^1D)$. The vibrational temperature of $N_2$ is important because it strongly influences important atmospheric characteristics such as electron density and temperature, and the quantity of infrared radiation from $CO_2$, $H_2O$, etc. The intersection of excited $N_2O$ triplet surfaces with the ground state singlet $N_2O$ surface will be determined, since these are central to understanding the vibrational deactivation of $N_2$ by $O(^1D)$. Preliminary SCF computations in our laboratory indicate that correlated MCSCF/CI wavefunctions are needed for these surfaces.

The reaction to form $NO^+(X^1\Sigma^+) + N(^4S)$ from $O^+(^4S) + N_2(X^1\Sigma^+)$ determines the free electron depletion rate in the ionosphere.[14] The understanding of this reaction involves the intersection of excited $N_2O^+$ quartet surfaces with the ground state $N_2O^+$ doublet surface. We shall investigate these in detail, since there may be reaction barriers which affect the accessible paths.

REFERENCES


1. R. S. Mulliken, Rev. Mod. Phys. **14**, 204 (1942).

2. A. D. Walsh, J. Chem. Soc. 2226 (1953).

3. F. C. Fehsenfeld, E. E. Ferguson, and A. C. Schmeltekopf, J. Chem. Phys. **45**, 1844 (1966).

4. F. Kauffman, J. Chem. Phys. **46**, 2449 (1967).

5. J. L. Moruzzi, J. W. Edin, and A. V. Phelps, J. Chem. Phys. **48**, 3070 (1968).

6. W. Lindinger, D. L. Albritton, F. C. Fehsenfeld, and E. E. Ferguson, J. Chem. Phys. **63**, 3238 (1976).

7. J. Comer and G. J. Schultz, Phys. Rev. **A10**, 2100 (1974).

8. W. E. Wentworth, E. Chen, and R. Freeman, J. Chem. Phys. **55**, 2075 (1971).

9. A. Zecca, I. Lazzizzera, M. Krauss, and C. E. Kuyatt, J. Chem. Phys. **61**, 4560 (1974).

10. T. G. Slanger and G. Black, J. Chem. Phys. **60**, 468 (1974).

11. R. F. Heidner, D. Husain, and J. R. Wiesenfeld, J. Chem. Soc. Faraday Trans. II, **69**, 927 (1973).

12. G. E. Zahr, R. K. Preston, and W. H. Miller, J. Chem. Phys. **62**, 1127 (1975).

13. J. C. Tully, J. Chem. Phys. **61**, 61 (1974).

14. A. D. Danilov, "Chemistry of the Ionosphere," (Plenum, New York, 1970).

Table 1. Bond dissociation energies and electron affinities for the $N_2O/N_2O^-$ systems. Units are eV.

| $D(N_2-O)$[a] | $D(N-NO)$[a] | $EA(O)$[b] | $EA(NO)$[c] | $D(N_2-O^-)$[d] | $EA(N_2O)$[e] | $D(N-NO^-)$[f] |
|---|---|---|---|---|---|---|
| 1.68 | 4.93 | 1.47 | 0.02 | 0.43 | 0.22 | 5.13 |

[a] G. Herzberg, "Electronic Spectra and Electronic Structure of Polyatomic Molecules," (Van Nostrand Reinhold, New York, 1966).

[b] R. S. Berry, Chem. Rev. **69**, 533 (1969).

[c] R. Celotta, R. Bennett, J. Hall, M. W. Siegel, and J. Levine, Bull. Am. Phys. Soc. **15**, 1515 (1970).

[d] D. G. Hopper, A. C. Wahl, R. L. C. Wu and T. O. Tiernan, J. Chem. Phys., in press.

[e] Equation (2a) of text

[f] Equation (2b) of text

Table 2. *Ab initio* potential energy surface characteristics for $N_2O^-$ and $N_2O$ .

| Parameter | $N_2O^-$ SCF | $N_2O^-$ MCSCF/CI | $N_2O$ MCSCF/CI | $N_2O$ Expt. |
|---|---|---|---|---|
| $R^e_{NN}$ (Å) | 1.204 | 1.222 | 1.147 | 1.128[a] |
| $R^e_{NO}$ (Å) | 1.376 | 1.375 | 1.240 | 1.184[a] |
| ∢NNO(deg) | 123.6 | 132.68 | 180 | 180[a] |
| $k_{NN}$ (md/Å) | 11.54 | 11.49 | 17.21 | 17.88[b] |
| $k_{NO}$ (md/Å) | 3.93 | 3.83 | 9.99 | 11.39[b] |
| $k_{NNO}$ (md/Å) | 0.645 | 0.643 | 0.41 | 0.49[b] |
| $\nu_{NO}$ $(cm^{-1})$[c] | 945 | 912 | 1223 | 1285[a] |
| $\nu_{NNO}$ $(cm^{-1})$[c] | 535 | 555 | 524 | 589[a] |
| $\nu_{NN}$ $(cm^{-1})$[c] | 1660 | 1666 | 2183 | 2224[a] |
| $\varepsilon_O$ (eV)[d] | 0.196 | 0.195 | 0.245 | 0.254[a] |

[a] G. Herzberg, "Electronic Spectra and Electronic Structure of Polyatomic Molecules" (Van Nostrand Reinhold, New York, 1966).

[b] E. B. Wilson, J. C. Decius, and P. C. Goss, "Molecular Vibrations" (McGraw-Hill, New York, 1955).

[c] Atomic masses are $m_N = 14.00751$, $m_O = 16.0000$

[d] Zero point energy.

Table 3. Bending and stretching barriers for $N_2O^-$

| | SCF | MCSCF/CI |
|---|---|---|
| $\Delta E_b$(eV)[a] | 1.41 | 1.10 |
| $\Delta E_s$(eV)[b] | -1.00 | -1.40 |
| $\Delta E$(eV)[c] | 2.41 | 2.50 |

[a]Energy rise upon bending ∢ (NNO) from the bent equilibrium value to 180°. Bondlengths are equal to their equilibrium values.

[b]Energy change upon stretching the NN and NO bondlengths from their equilibrium $N_2O$ values to their equilibrium $N_2O^-$ values.

[c]$\Delta E = \Delta E_b - \Delta E_s$

# IONS OF NITROGEN DIOXIDE

## A. Introduction

High resolution photoelectron spectra for $NO_2$ are known for energies up to 27.5 eV.[1,2] The $NO_2^+$ ion peaks have been assigned on the basis of ground state $NO_2^+$ calculations and by analogy with the isoelectronic $CO_2$ molecule.[2-4] No definitive experimental assignment of the first ionization potential has been made, owing to the great difference between the neutral (bent) and ion (linear) equilibrium geometries.

Semiempirical calculations on $NO_2^-$ [5,6] are in essential agreement with a number of experiments dealing with absorption spectra in $NaNO_2$ or phosphorescence in aqueous solutions. Polarization studies have assigned the electric dipole allowed $^1B_1$ state in the region just under 3 eV.[7,8] The $^3B_1$ state has been assigned to $\sim$2.4 eV.[9-11] The $^1A_2$ state was calculated to be $\sim$4.5 eV semiempirically,[5] and on this basis spectral assignments made.[10,12,13] The $^1B_2$ state is dipole allowed, and lies about 6 eV above $X\,^1A_1$.[5,12]

## B. Neutral $NO_2$

The most accurate theoretical results available for $NO_2$ were previously calculated in this laboratory.[14] We use these to evaluate our present efforts for the singly charged ions. The vertical $NO_2$ spectrum we compute agrees with the accurate results to within $\sim$0.6 eV. To the extent that $NO_2$ is representative of $NO_2^+$ and $NO_2^-$, a comparable accuracy of the ionic spectra is expected.

C. Positive Ion $NO_2^+$

Vertical excitation energies for $NO_2$ ($R_{NO}$ = 2.25 bohrs, $\sphericalangle$ ONO = 134°) were computed with single- and multiconfiguration self-consistent-field methods (SCF and MCSCF methods). Configuration interaction was then carried out using the MCSCF results (MCSCF/CI). The computed and experimental spectra are compared in Table 1. The SCF results predict the wrong first ionization potential ($^3B_2$ instead of $^1A_1$), but otherwise are in reasonable agreement with the MCSCF/CI spectrum. The MCSCF/CI spectrum is somewhat different from the experimental spectrum, and this may in part be due to the difference between theoretically computed vertical ionizations and those obtained by subtracting experimental photoelectron spectral peaks. This is probable for molecules like $NO_2/NO_2^+$, where ground state neutral and ion equilibrium geometries are very different. Because of these geometry differences, vibrationally excited levels can be expected to be observed in the experiments, and these are not included in theoretical calculations such as ours.

A linear to bent geometry $NO_2^+$ correlation diagram is drawn on Figure 1. The energies represented by solid lines are SCF energies. The dashed lines represent MCSCF variational estimates of states which collapse variationally in the SCF model. The dotted line shown for ($^1B_2$) should not be taken too seriously, since it is a guess made on the basis of the Walsh-Mulliken rules,[15-16] and was not observed in our computed results. The linear $NO_2^+$ SCF spectrum appears to be correctly ordered, and clearly shows the greater stability of the linear ground state. However, the behavior of the states introduced by bending is not like that observed in $CO_2$, and this is possibly significant because in the past orderings, etc., have been rationalized by assuming $CO_2$ is a reasonable model for $NO_2^+$.

D. Negative Ion $NO_2^-$

Computed SCF vertical excitation energies ($R_{NO}$ = 2.25 bohrs, $\sphericalangle$ ONO = 134°) and experimental excitation energies for $NO_2^-$ are shown in Table 2. Qualitative agreement is observed between the SCF and experimental spectra, but quantitative differences are obvious. Reasons for the quantitative differences may in part be due to differences between the vertical geometry and the experimental geometry. For example, the $\sphericalangle$ ONO for the minimum $X^1A_1$ geometry may be $\sim$ 116°[17,18] as opposed to the vertical value $\sphericalangle$ ONO = 134°. Another possible reason is that the SCF method is not totally appropriate for the kinds of vertical electron attachments that occur in forming $NO_2^-$ from $NO_2$.

An adiabatic correlation diagram for $NO_2^-$ is drawn on Figure 2. The $C_{2v}$ energy levels are those reported in Table 2. The diagram on Figure 2 is the first for $NO_2^-$ that is based on *ab initio* energy levels.

According to the correlation diagram, electron attachment in the range $\sim$0-1 eV is associated with only two states, $^3B_1$ and $X^1A_1$. Structure which is observed below 1 eV should be associated with the ground state, in agreement with experimental conclusions.[19-21] Dissociative attachment of electrons has produced each of the species $O^-$, $O_2^-$ and $NO^-$.[22-24] The appearance potentials for each are about the same as their thermodynamic thresholds. The adiabatic paths on Figure 2 likewise suggest no apparent barriers. The production of $O^-$ is observed to be largest,[22] and this agrees with the fact that several adiabatic paths on Figure 2 provide routes to the lowest energy asymptote, which produces $O^-$. However, non-adiabatic interactions must occur for the case of $NO^-$ production.

## E. Future Goals

The SCF linear to bent geometry correlation diagrams for $NO_2^+$ and $CO_2$ which we have computed in the present work suggest that the isoelectronic $CO_2$ and $NO_2^+$ molecules behave differently in a qualitative sense. We shall determine whether this difference prevails in more accurate descriptions. Several of the states which enter in $NO_2^+$ Walsh rules will also be computed in order to furnish a completely *ab initio* correlation diagram. The extended and more accurate descriptions of $NO_2^+$ will also be needed to further understand the difference between theory and experiment, if indeed this difference persists.

Negative ion $NO_2^-$ energy levels which include electron correlation, as well as different bending angles, are likewise needed to clarify the differences between theory and experiment. In this respect $NO_2^-$ is a good candidate system, since it is variationally stable relative to $NO_2$ in many states, and since, experimentally, optically allowed transitions are low-lying in the $NO_2^-$ spectrum.

## REFERENCES


1. O. Edqvist, E. Lindholm, L. E. Selin, L. Asbrink, C. E. Kuyatt, S. R. Mielczarek, J. A. Simpson, and I. Fischer-Hjalmars, Physical Scripta **1**, 172 (1970).
2. C. R. Brundle, D. Neumann, W. C. Price, D. Evans, A. W. Potts, and D. G. Streets, J. Chem. Phys. **53**, 705 (1970).
3. K. L. McEwen, J. Chem. Phys. **32**, 1801 (1960).
4. L. Burnelle, P. Beaudoin, and L. J. Schaad, J. Phys. Chem. **71**, 2240 (1967).
5. K. L. McEwen, J. Chem. Phys. **34**, 547 (1961).
6. H. J. Maria, D. Larson, M. E. McCarville, and S. P. McGlynn, Accts. Chem. Res. **3**, 368 (1970).
7. J. W. Sidman, J. Amer. Chem. Soc. **79**, 2669 (1957).
8. J. W. Sidman, J. Amer. Chem. Soc. **79**, 2675 (1957).
9. H. J. Maria, A. Wahlborg, and S. P. McGlynn, J. Chem. Phys. **49**, 4925 (1968).
10. R. M. Hochstrasser and A. P. Marchetti, J. Chem. Phys. **50**, 1727 (1969).
11. W. C. Allen and R. N. Dixon, Trans. Faraday Soc. **65**, 1168 (1969).
12. W. G. Trawick and W. H. Eberhardt, J. Chem. Phys. **22**, 1462 (1954).
13. L. E. Harris, H. J. Maria, and S. P. McGlynn, Czech. J. Phys. **B20**, 1007 (1970).
14. G. D. Gillispie, A. U. Khan, A. C. Wahl, R. P. Hosteny, and M. Krauss, J. Chem. Phys. **63**, 3425 (1975).
15. R. S. Mulliken, Rev. Mod. Phys. **14**, 204 (1942).
16. A. D. Walsh, J. Chem. Soc. 2226 (1953).
17. R. Kato and J. Rolfe, J. Chem. Phys. **47**, 1901 (1967).
18. D. E. Milligan, M. E. Jacox, and W. A. Guillory, J. Chem. Phys. **52**, 3864 (1970).
19. M. J. W. Boness, J. B. Hasted, and I. W. Larkin, Proc. Roy. Soc. (London), **A305**, 493 (1968).
20. I. W. Larkin and J. B. Hasted, J. Phys. **B5**, 95 (1972).

<u>REFERENCES</u>, Cont'd.

21. L. Sanche and G. J. Schultz, J. Chem. Phys. **58**, 479 (1973).

22. J. F. Paulson, Adv. Chem. Ser. 80, 28 (1966). (R. F. Gould, ed., J. Amer. Chem. Soc., Washington).

23. J. A. D. Stockdale, R. N. Compton, G. S. Gurst, and P. W. Reinhardt, J. Chem. Phys. **50**, 2176 (1969).

24. R. E. Fox, J. Chem. Phys. **32**, 285 (1960).

Table 1. Vertical excitation energies for $NO_2^+$, $R_{NO}$ = 2.24 bohrs, ∢ ONO = 134°. Units are eV.

| Ion State | SCF | MCSCF/CI | Expt.[a] |
|---|---|---|---|
| $^1A_1$ | 0.90 | 0.00 | 0.00 |
| $^3B_2$ | 0.00 | 2.56 | 1.78 |
| $^3A_2$ | 1.34 | 2.65 | 2.37 |
| $^1A_2$ | 1.78 | 3.55 | 2.83 |
| $^1B_2$ | 4.13 | 3.84 | 3.28 |
| $^3A_1$ | 7.28 | 6.83 | 6.22 |
| $^3B_1$ | 8.27 | 7.70 | 6.41 |
| $^1B_1$ | 9.28 | 8.78 | - |

[a] C. R. Brundle, D. Neumann, W. C. Price, D. Evans, A. W. Potts, and D. G. Streets, J. Chem. Phys. **53**, 705 (1970).

Table 2. Excitation energies for $NO_2^-$, $R_{NO}$ = 2.25 bohrs, ∢ ONO = 134°. Units are eV.

| Ion State | SCF[a] | Expt.[b] |
|---|---|---|
| $^1A_1$ | 0.00 | |
| $^3B_1$ | 0.98 | ∿2.4[c-e] |
| $^1B_1$ | 2.47 | ∿3[f,g] |
| $^3B_2$ | 4.12 | |
| $^3A_2$ | 5.60 | |
| $^1A_2$ | 5.92 | ∿4.5[h] |
| $^1B_2$ | 8.26 | ∿6[d,i,j] |
| $^3A_1$ | 9.62 | |

[a] Vertical

[b] Adiabatic

[c] H. J. Maria, A. Wahlborg, and S. P. McGlynn, J. Chem. Phys. **49**, 4925 (1968).

[d] R. M. Hochstrasser and A. P. Marchetti, J. Chem. Phys. **50**, 1727 (1969).

[e] W. C. Allen and R. N. Dixon, Trans. Faraday Soc. **65**, 1168 (1969).

[f] J. W. Sidman, J. Amer. Chem. Soc. **79**, 2669 (1957).

[g] J. W. Sidman, J. Amer. Chem. Soc. **79**, 2675 (1957).

[h] K. L. McEwen, J. Chem. Phys. **34**, 547 (1961).

[i] W. G. Trawick and W. H. Eberhardt, J. Chem. Phys. **22**, 1462 (1954).

[j] L. E. Harris, H. J. Maria, and S. P. McGlynn, Czech. J. Phys. **B20**, 1007 (1970).

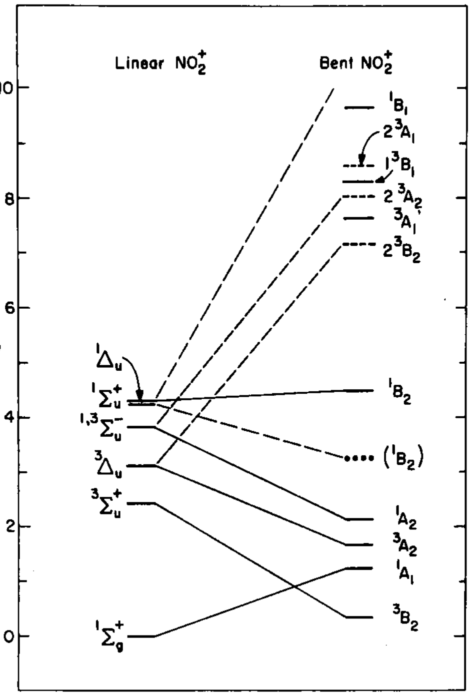


Fig. 1.

State Correlation Diagram for Linear and Bent NO$^+$. The Solid Lines are SCF Energy Levels. The Dashed Lines are Variational MCSCF Values for Higher Roots of a Given Symmetry. The Dotted Value is an Estimate Based on the Walsh-Mulliken Rules, and was not Computed *ab initio*. The Energy Zero is $NO_2^+(^1\Sigma_g^+)$ as Given by the SCF Model.

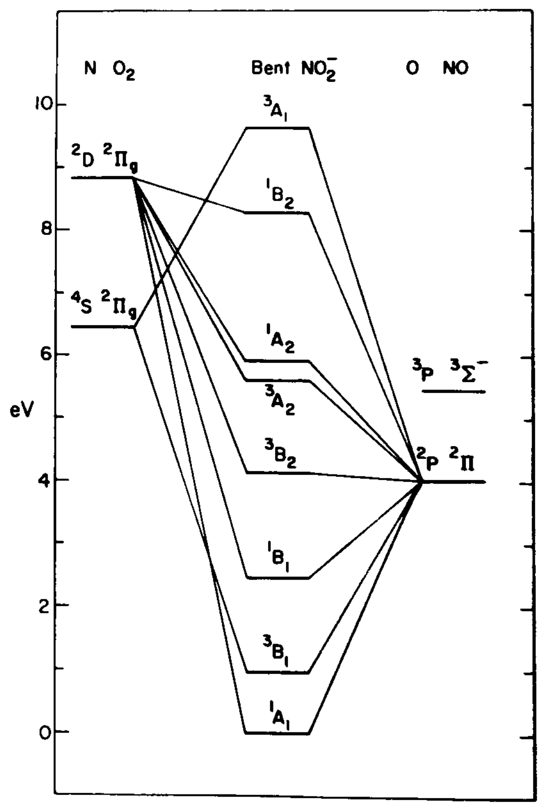


Fig. 2.

State Correlation Diagram for $NO_2^-$. The Molecular Ion Energies are SCF Values. The Asymptote Energies were taken from "Potential Energy Surfaces for Air Triatomics," M. Krauss, D. G. Hopper, P. J. Fortune, A. C. Wahl, and T. O. Tiernan, ARL TR 75-0202, Vol. 1. The Energy Zero is $NO_2^-(^1A_1)$ as Given by the SCF Model.